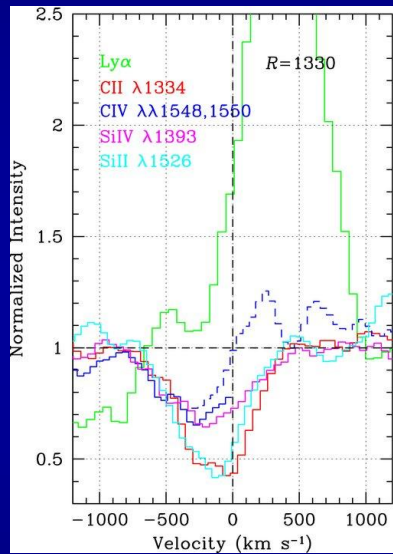
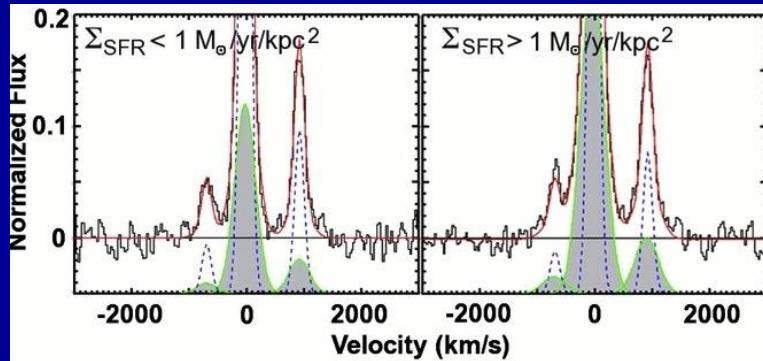


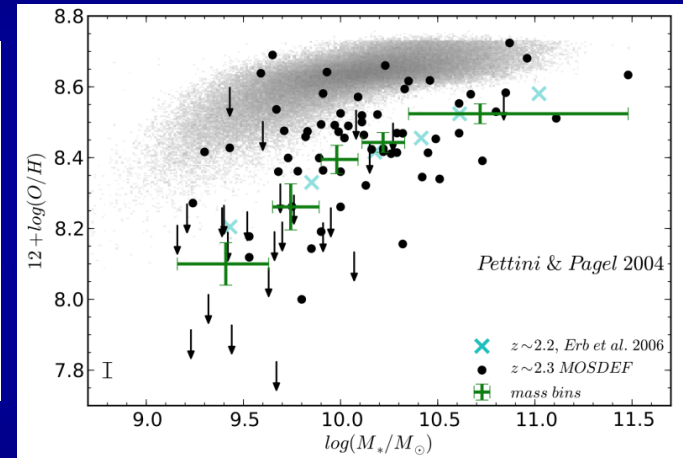
Outflows from High-Redshift Galaxies



Steidel et al. (2010)



Newman et al. (2012b)



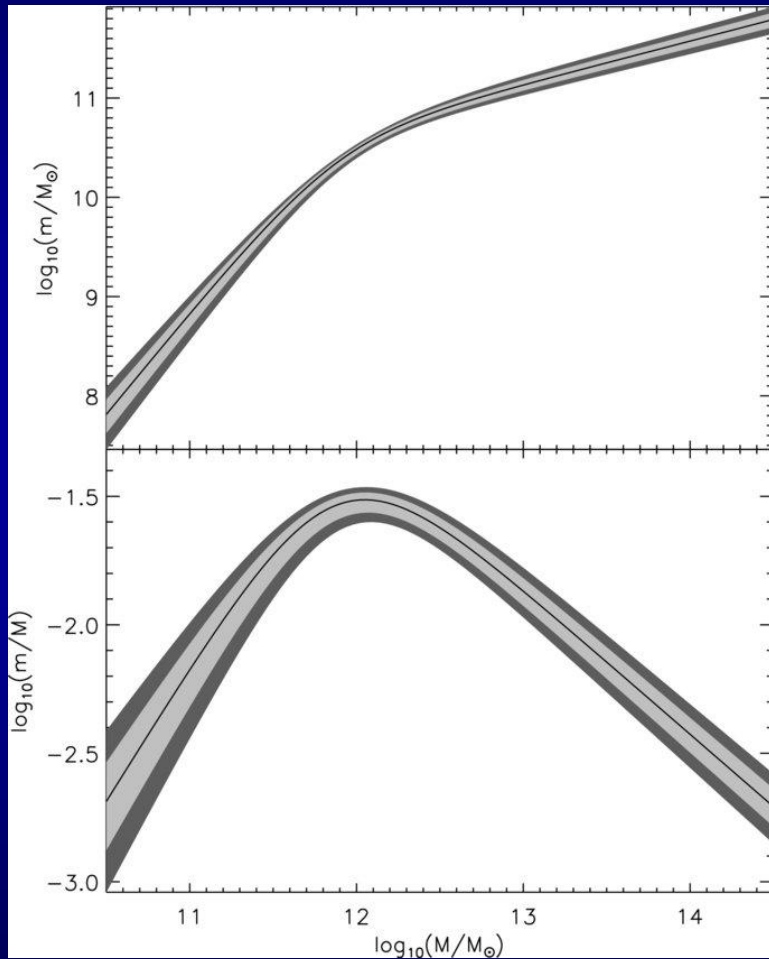
Sanders et al., in prep

Alice Shapley (UCLA)

Overview

- **Importance of outflows**
- **Properties of outflows**
- **Direct Probes of Outflows at High Redshift ($z \sim 1-4$)**
 - **Measurements**
 - **Mass outflow rates**
 - **Outflow scaling relations and “demographics”**
 - **Outflow geometry**
 - **Evolution**
- **M-Z relation and the MOSDEF project**
- **Concluding thoughts**

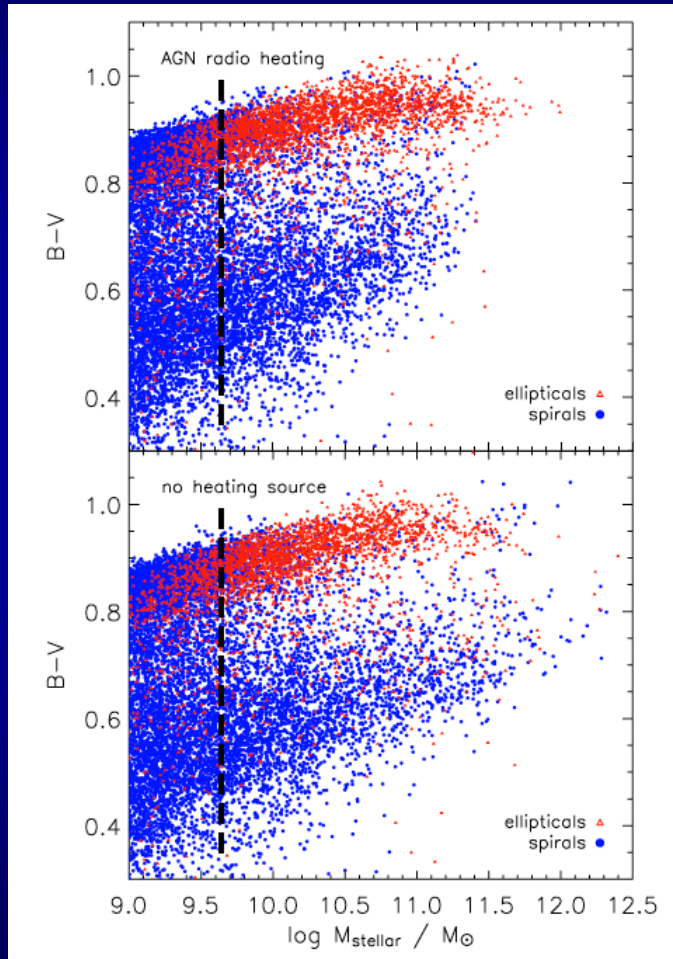
Importance of Outflows



(Moster et al. 2010)

- Feedback processes are key to successful models of galaxy formation and the IGM.
- Stellar vs. halo masses, especially at low and high-mass end.
- Red colors of massive galaxies at $z \sim 0$.
- The enrichment of the IGM.
- Outflows are observed in local starbursts, and, commonly, at $z > 1$.

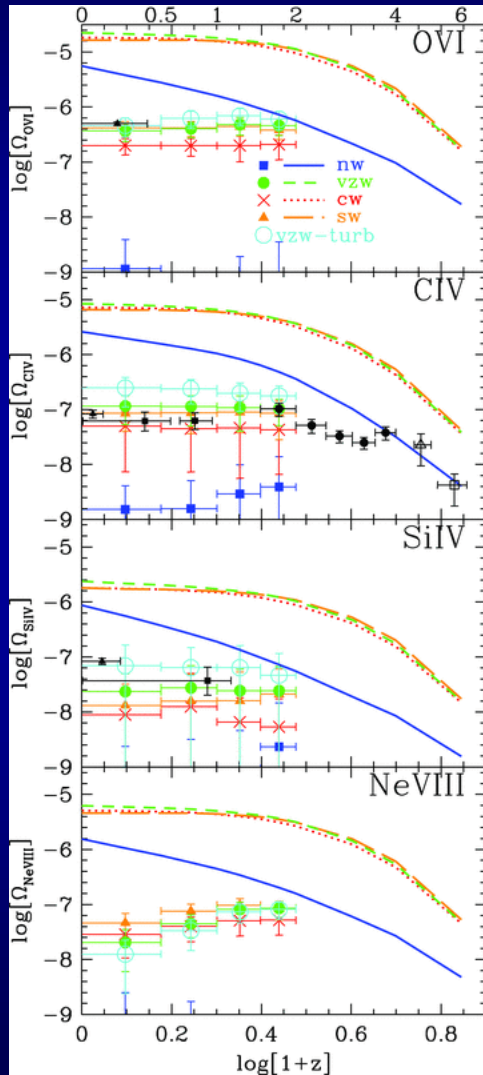
Importance of Outflows



(Croton et al. 2006)

- Feedback processes are key to successful models of galaxy formation and the IGM.
- Stellar vs. halo masses, especially at low and high-mass end.
- Red colors of massive galaxies at $z \sim 0$.
- The enrichment of the IGM.
- Outflows are observed in local starbursts, and, commonly, at $z > 1$.

Importance of Outflows



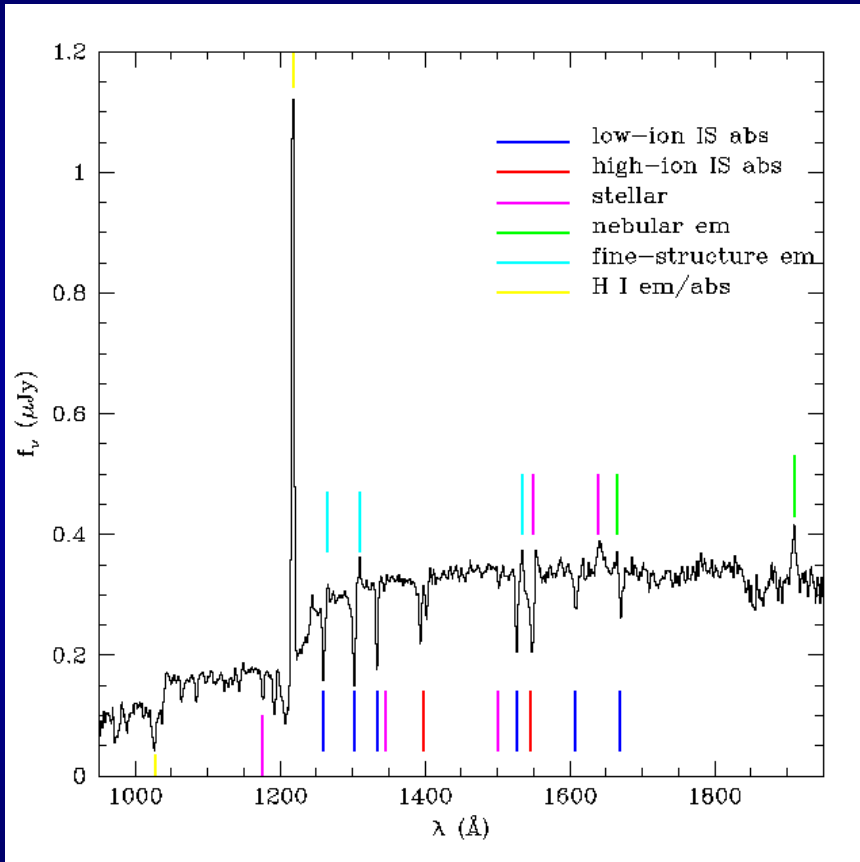
(Oppenheimer et al. 2012)

- Feedback processes are key to successful models of galaxy formation and the IGM.
- Stellar vs. halo masses, especially at low and high-mass end.
- Red colors of massive galaxies at $z \sim 0$.
- The enrichment of the IGM.
- Outflows are observed in local starbursts, and, commonly, at $z > 1$.

Properties of Outflows

- Mass outflow rates (e.g., $\dot{M}_{\text{wind}} = \Omega r^2 \rho v$)
- Mass loading factor: $\eta = \dot{M}_{\text{wind}} / \text{SFR}$
 - Scaling with galaxy mass or circular velocity
 - Discriminate between “momentum driven” ($\eta \sim 1/v_c$) and “energy driven” ($\eta \sim 1/v_c^2$) winds
 - Scaling with other galaxy properties (e.g., Σ_{SFR})
- Metal loading factor: $\zeta = Z_{\text{wind}} / Z_{\text{ISM}} \times \eta$ and scaling with mass
- Multi-phase structure and mass in each phase
- Geometry (e.g., bipolar or spherical, physical extent)
- Velocity structure (v_{wind} vs. r)
- Outflow kinematics vs. galaxy properties
- Fate of outflowing gas (v_{wind} vs. v_{esc})

$z > 2$ Outflow Features



- In star-forming galaxies at $z > 2$, a host of rest-frame UV features within the range $\sim 1200\text{-}2000 \text{\AA}$ is used to trace outflows:
 - HI Ly α absorption and emission.
 - Low-ionization interstellar absorption lines (SiII, OI, CII, FeII, AlII) probing cool, neutral phase.
 - High-ionization interstellar absorption lines (SiIV, CIV) probing warmer, more highly ionized phase.
 - Potential to estimate HI column directly!

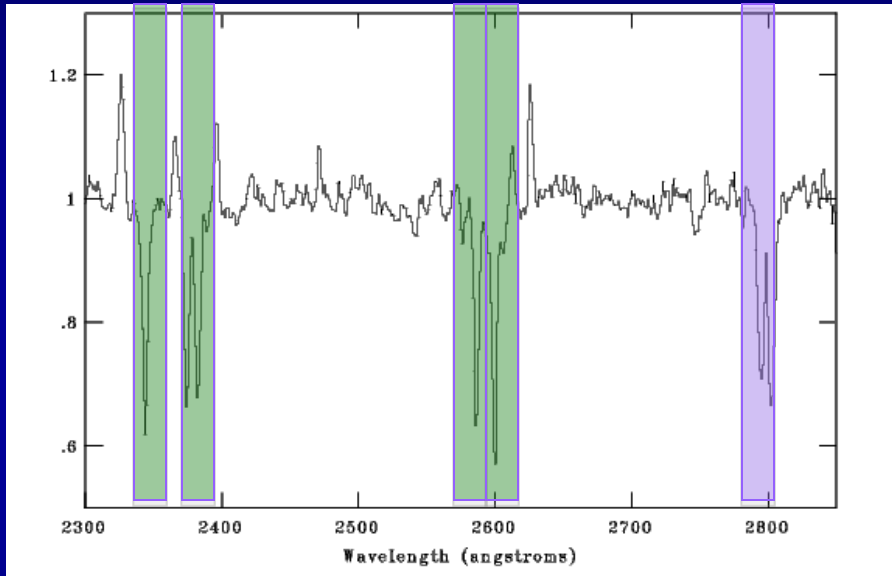
(Shapley et al. 2003)

z~1 Outflow Features

FeII

FeII

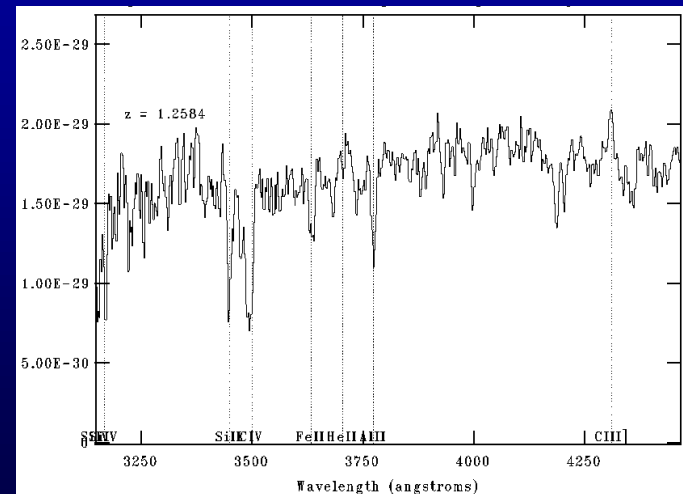
MgII



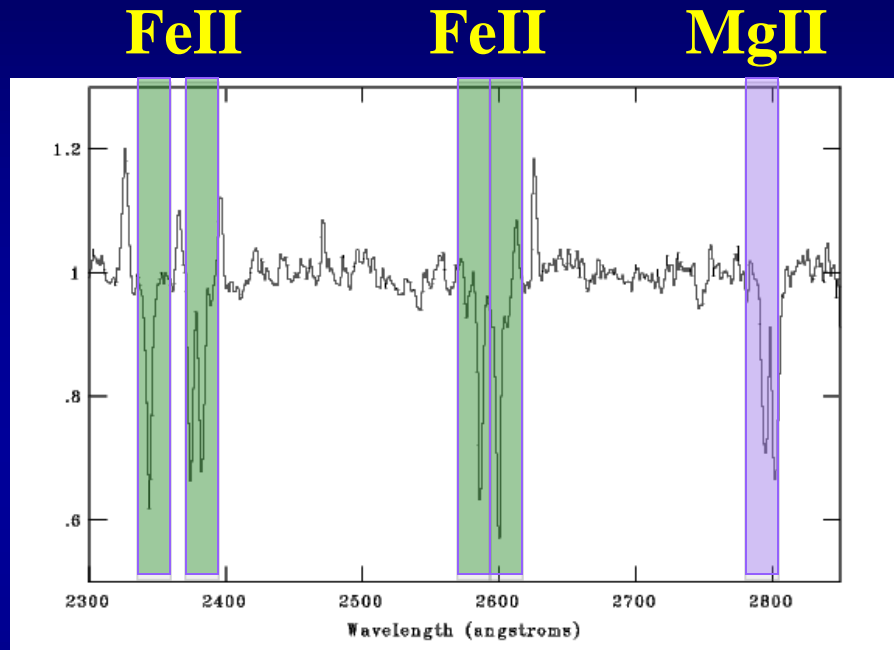
• In galaxies at $z\sim 0.5-1.5$, use near-UV features:

- **FeII**: FeII $\lambda 2250$, $\lambda 2261$, $\lambda 2344$, $\lambda 2374$, $\lambda 2382$, $\lambda 2587$, $\lambda 2600$ Å.
- **MgII** doublet $\lambda\lambda 2796, 2803$.
- **MgI** $\lambda 2852$.
- **Probe cool gas.**
- **Can use CIV, SiII, AlII as well, at $z>1.1$ with Keck/LRIS.**

(Weiner et al. 2009; Rubin et al. 2010a,b; 2011, 2012, 2013; Martin, AS et al. 2012, 2013; Kornei, AS et al. 2012, 2013.)



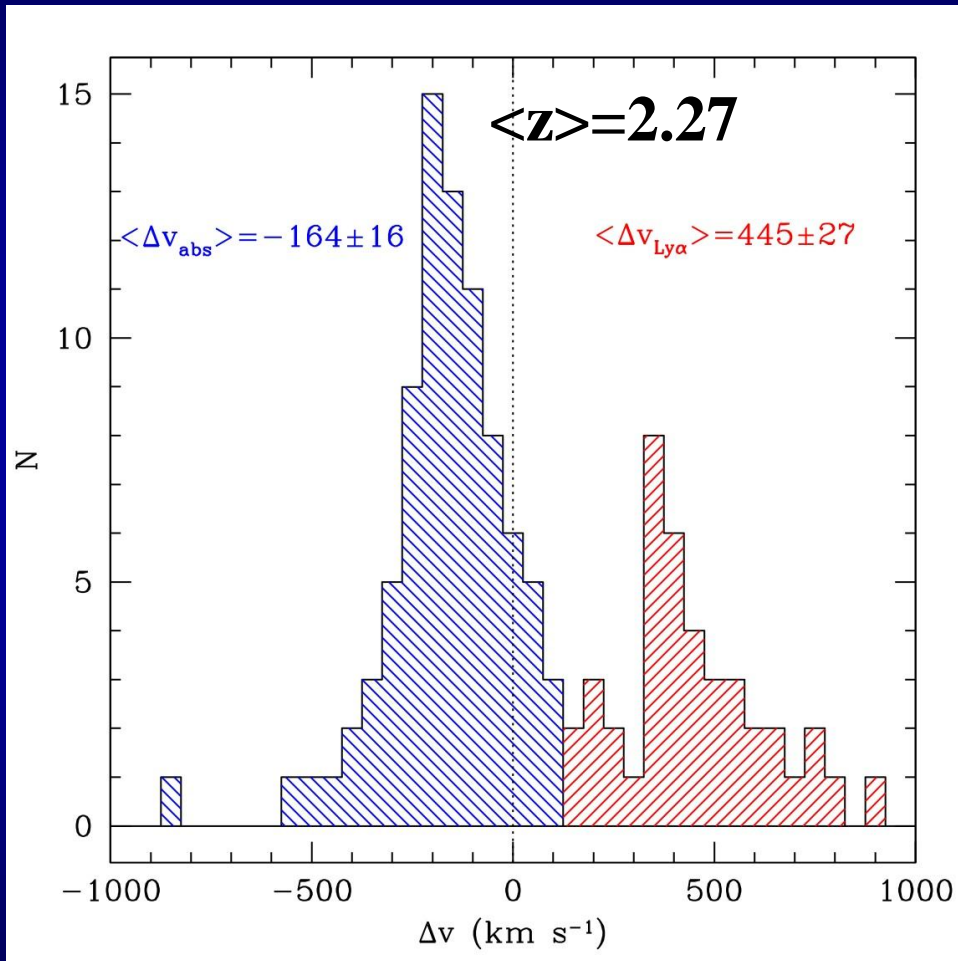
Quantifying an “Outflow”



(Weiner et al. 2009; Rubin et al. 2010a,b; 2011, 2012, 2013; Martin, AS et al. 2012, 2013; Kornei, AS et al. 2012, 2013.)

- Different methods for estimating outflow properties:
 - Velocity centroid of single-component fit
 - Decomposition into ISM+outflow components, velocity centroid of outflow component
 - EW of outflow component
 - Blue wing of single/outflow component
 - Full velocity profile
- Resolution of data is very important.

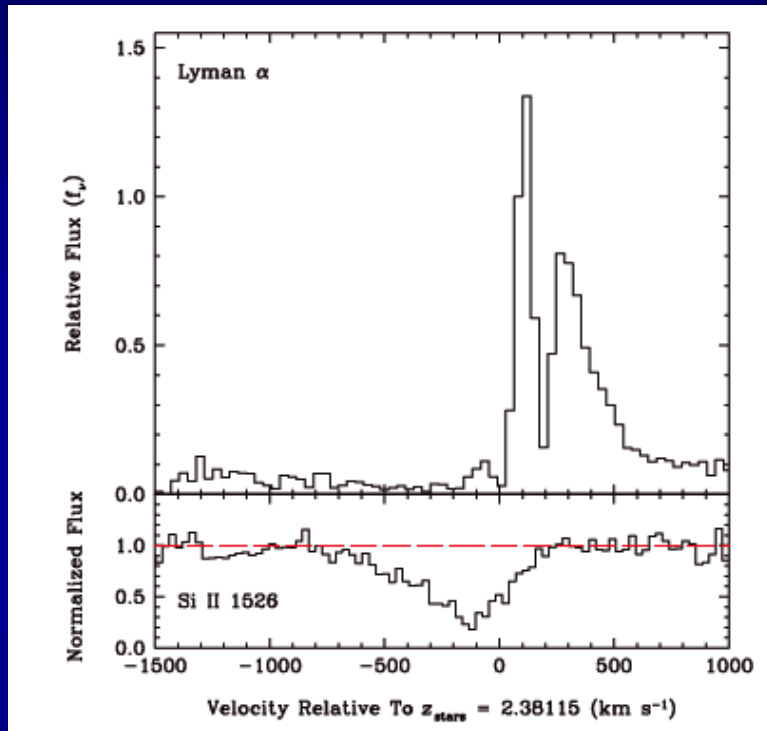
Systemic Redshifts



(Steidel et al. 2010)

- **Kinematic signature: Redshifts measured for interstellar absorption, Ly α emission differ.**
- **At $z \sim 2-3$, systemic redshifts indicate: Low-ionization absorption features typically blueshifted ($\Delta v = -150$ km/s), Ly α emission typically redshifted ($\Delta v = +400-500$ km/s).**
- **E.g., 89 galaxies at $\langle z \rangle = 2.3$ with Keck/NIRSPEC systemic redshifts, and rest-UV spectra (Steidel et al. 2010)**
- **Keck/MOSFIRE will dramatically increase sample with systemic redshifts (e.g., Erb et al. 2014).**

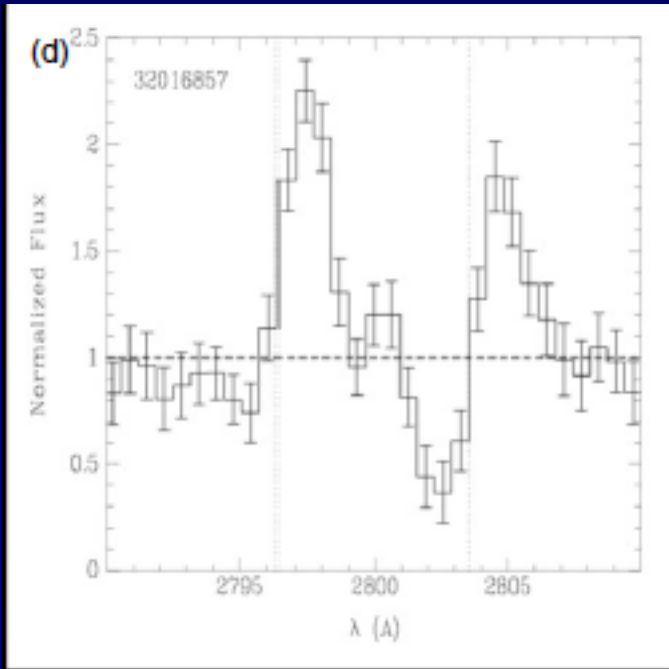
Resonant UV Emission Lines



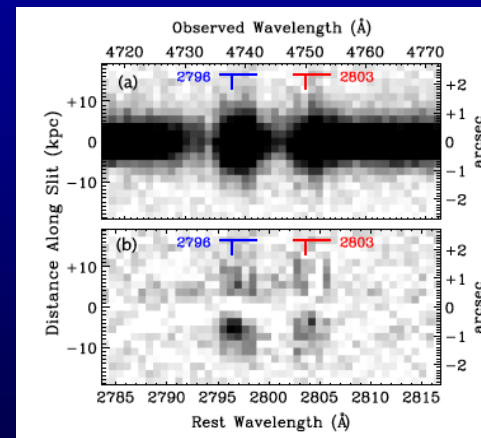
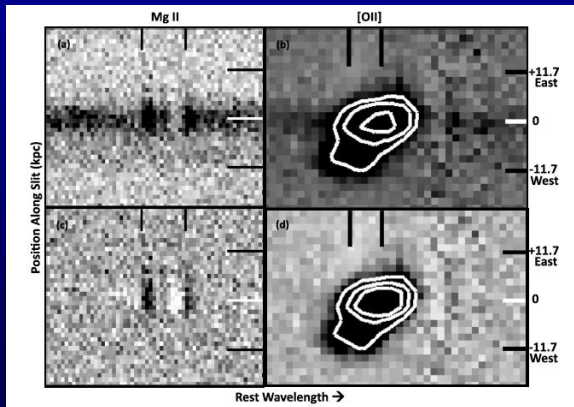
“Cosmic Horseshoe”, $z=2.38$
(Quider et al. 2009)

- Resonant Ly α emission, typically redshifted.
- Velocity structure of line should contain rich information about geometry, column density, and velocity structure of outflow (or inflow). See models by Verhamme, Schaerer et al.
- Angular extent also contains important clues (Steidel et al. 2011).
- Issue: most observations of unlensed high- z galaxies have velocity resolution coarser than ~ 200 km/s (typical is ~ 400 - 500 km/s), which limits ability to compare with model velocity profiles.

Resonant UV Emission Lines



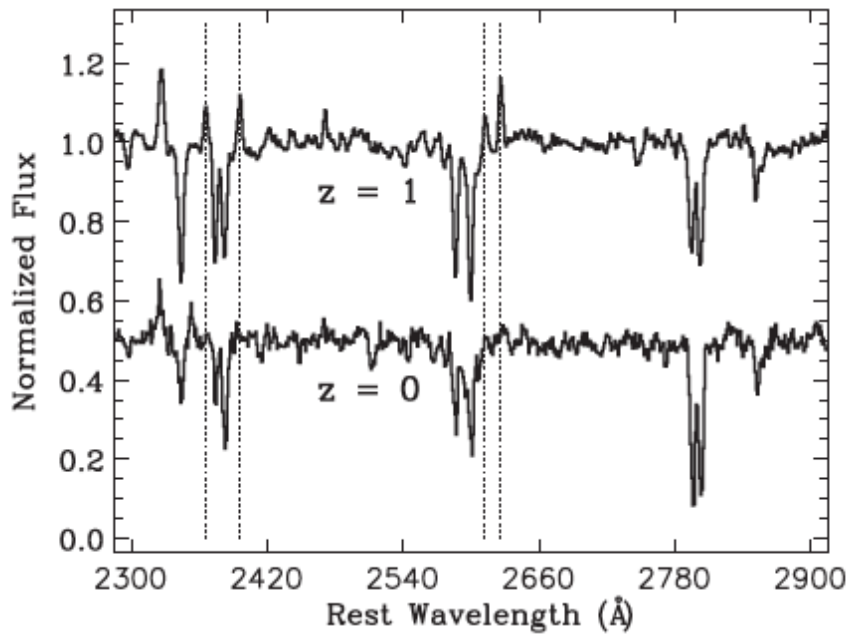
- Resonant MgII emission, typically redshifted.
- At least a couple of cases where MgII is spatially extended relative to the continuum, with different velocity structure from that of [OII] emission.
- Useful target for IFU measurements.



(Rubin et al. 2013)

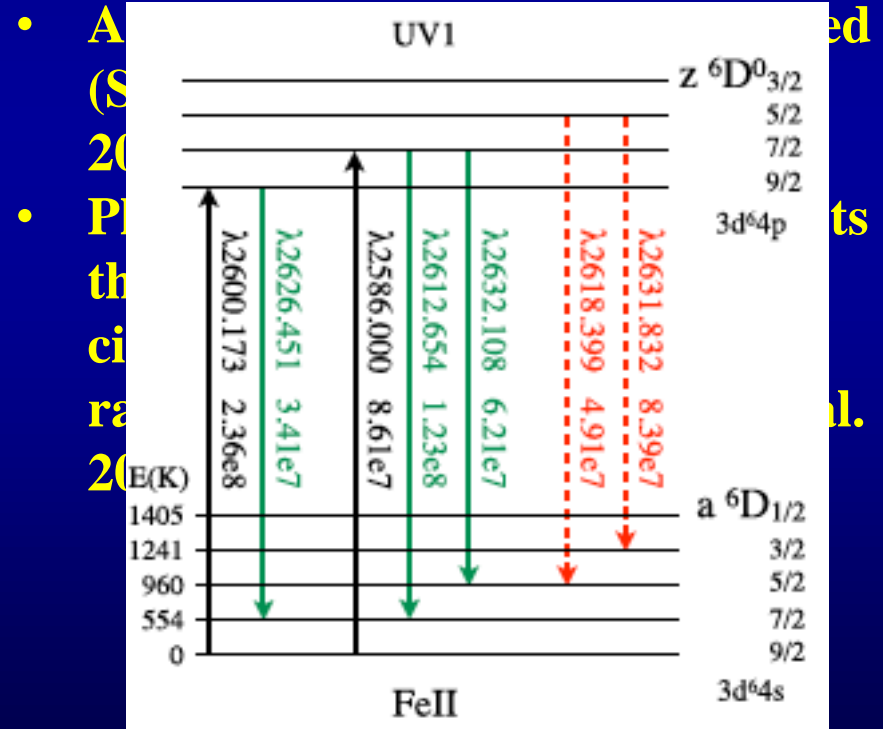
(Martin et al. 2013)

Fine Structure UV Emission Lines



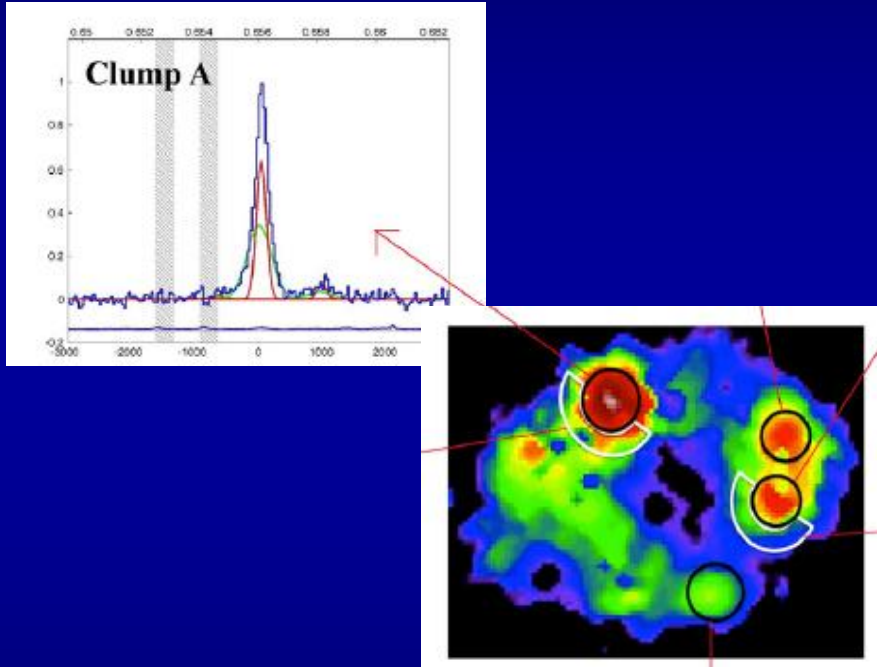
(Kornei, AS et al. 2013)

- FeII* emission not seen in composite UV spectrum of local starbursts (Leitherer et al. 2010). Commonly detected at $z > 1$, generic prediction given FeII energy levels.



Broad H α Emission

- VLT/SINFONI IFU maps of H α from star-forming galaxies at $z \sim 2$.
- Decompose H α profiles into double-Gaussian fits.
- Broad H α emission components (sometimes systematically blueshifted) associated with “clumps” and nuclei, interpreted as outflows.



ZC406690 ($z=2.19$), H α map

(Newman et al. 2012a,b;
Genzel et al. 2011, Forster
Schreiber et al. 2014)

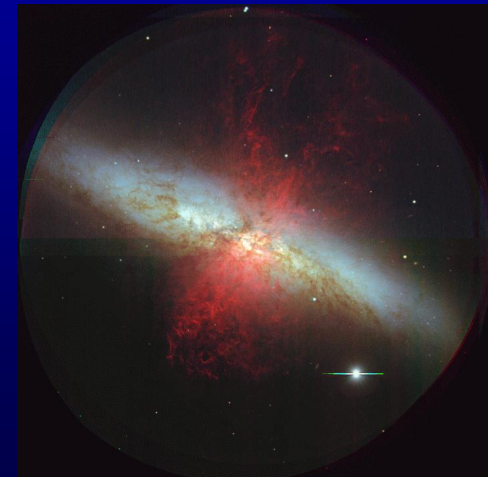


(Image credit: Subaru Observatory)

Mass Outflow Rates

- Expression for outflow rate:

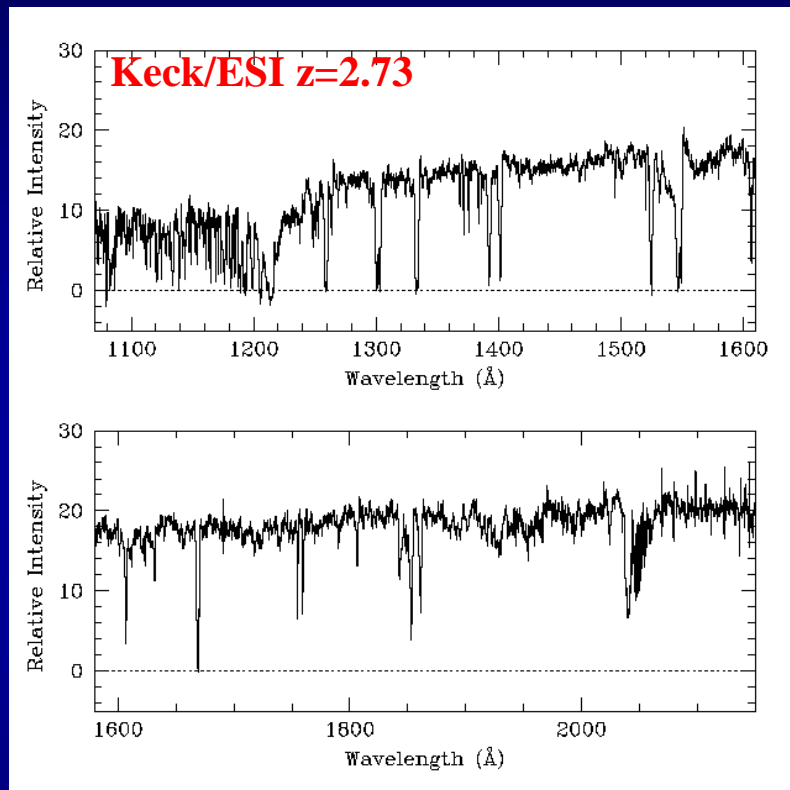
$$\dot{M}_w = \Omega r^2 \mu(r) n(r) v(r),$$

- For absorption measurements, use column density $N(\text{HI})$, to rewrite as:

$$\dot{M}_w \approx \Omega R_0 m_p N_{\text{HI}} v_\infty$$

- Need to estimate Ω (covering factor), R_0 (radius at which wind is measured), N_{HI} , in addition to v_∞ (terminal velocity)

Mass outflow rates at $z > 2$: Absorption

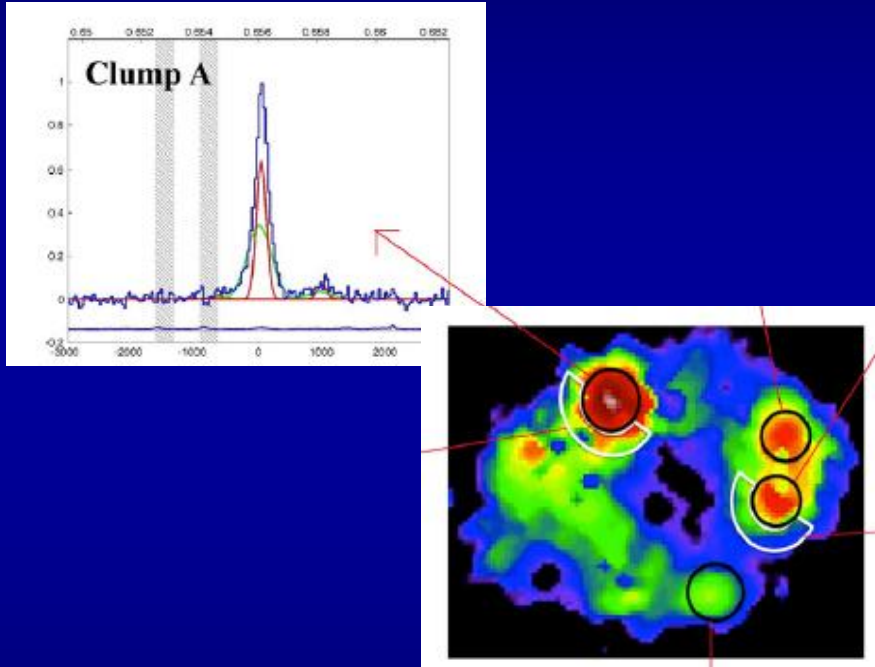


cb58 has non-average spectrum -- very strong Ly α and metal absorption lines

- MS1512-cB58, $z=2.73$, x30 magnification, R-mag ~ 20.5 (Yee et al. 1996). Detailed studies of outflowing ISM, abundance pattern, multi-wavelength follow-up, very strong absorption lines (Pettini et al. 2000, 2002).

- For 10 years, this was the *only* LBG with a mass outflow estimate, where $dM/dt \sim SFR$, based on N_{HI} , v_{out} , $\Omega=4\pi$, assumption of $R=1kpc$

Mass outflow rates at $z > 2$: Emission



ZC406690 ($z=2.19$), H α map

(Newman et al. 2012a;
Genzel et al. 2011)

- Broad component of clump H α profiles used to estimate mass outflow rates and mass loading factor:

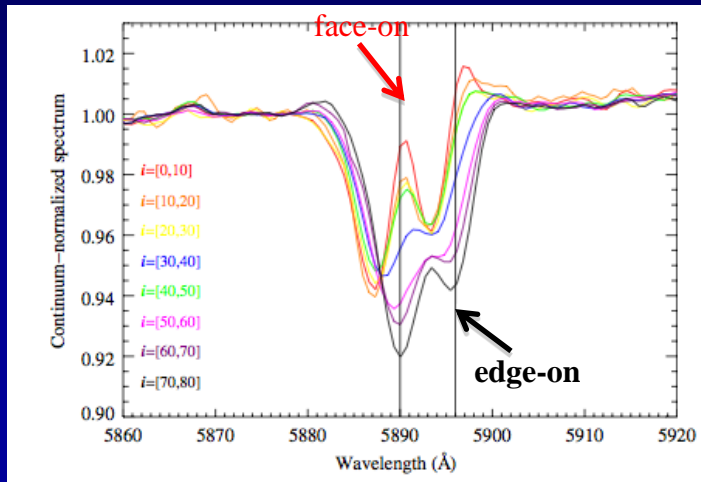
$$L_{\text{H}\alpha} = \gamma_{\text{H}\alpha} \int \Omega R^2 n_e(R) n_p(R) dR,$$

$$M_{\text{H II, He}} = 1.36 \times m_p \int \Omega R^2 n_p dR = \frac{1.36 \times m_p L_{\text{H}\alpha}}{\gamma_{\text{H}\alpha} n_{\text{eff}}},$$

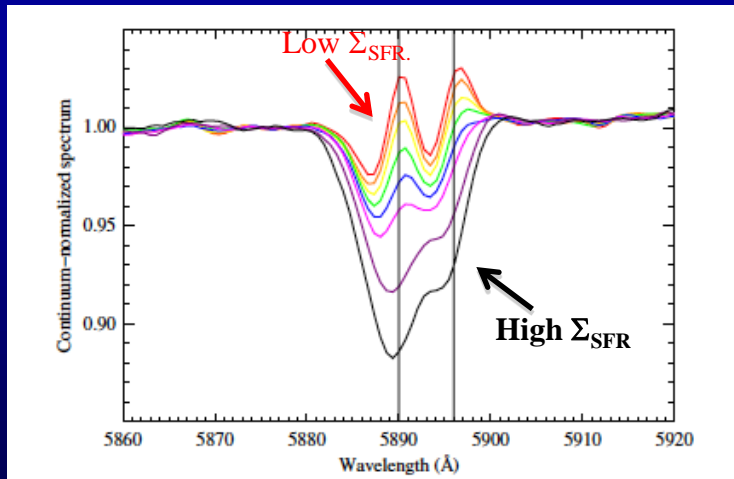
$$\dot{M}_{\text{out}} = \Omega R^2 1.36 \times m_p n(R) v_{\text{out}} = M_{\text{H II, He}} \times \frac{v_{\text{out}}}{R_{\text{out}}}$$

- $\dot{M}_{\text{out}} \sim L_{\text{H}\alpha} / n_{\text{eff}} \times v_{\text{out}} / R_{\text{out}}$
- Major uncertainty is density distribution of wind, R_{out} . Conclude $\dot{M}_{\text{out}} \sim \text{SFR}$ (i.e. $\eta \sim 1$), but *extremely* uncertain (e.g., $\eta = 2.9^{+27.6}_{-2.5}$).

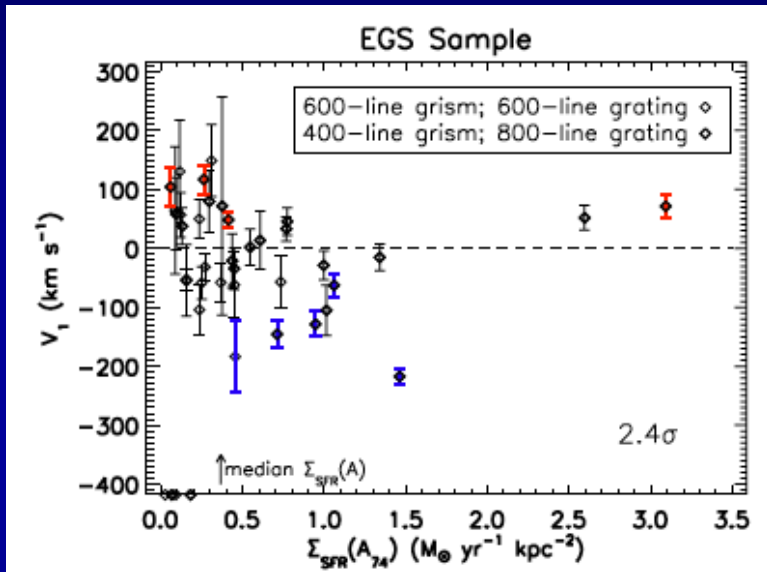
z~0 Outflow Kinematic Trends



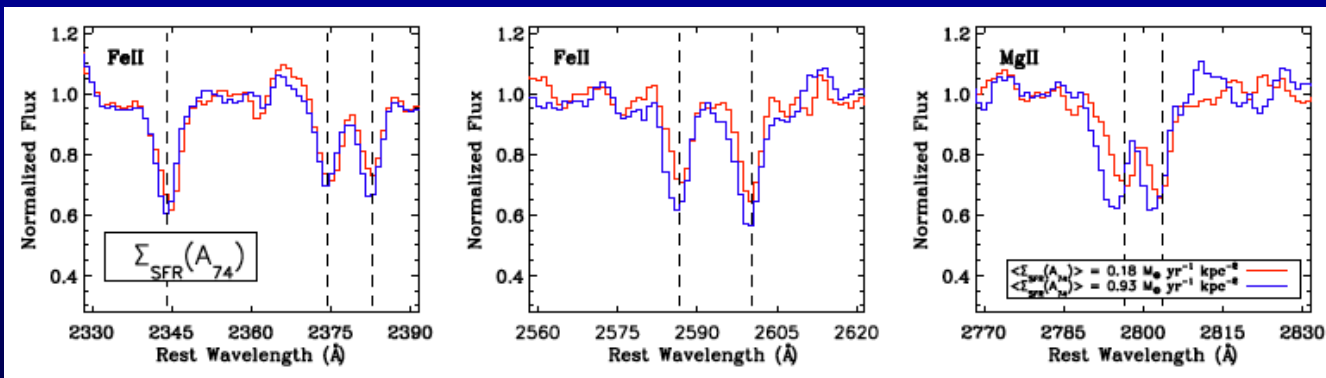
- ~140,000 galaxies drawn SDSS DR7, $z_{\text{med}} \sim 0.09$, $\text{SFR} \sim 1 M_{\odot}/\text{yr}$.
- Stack according to inclination, SFR, Σ_{SFR} , A_{UV} , M^* . Correct Na I spectra for both stellar and systemic ISM component.
- Outflow component more prevalent in face-on galaxies.
- Outflow component EW correlates primarily with Σ_{SFR} and then A_{UV} . Amount of material propelled in outflow depends on Σ_{SFR} .
- Shallow trend of v_{out} with Σ_{SFR} , with $|v_{\text{out}}| \sim \Sigma_{\text{SFR}}^{0.1}$.



Outflow kinematics at $z \sim 1$

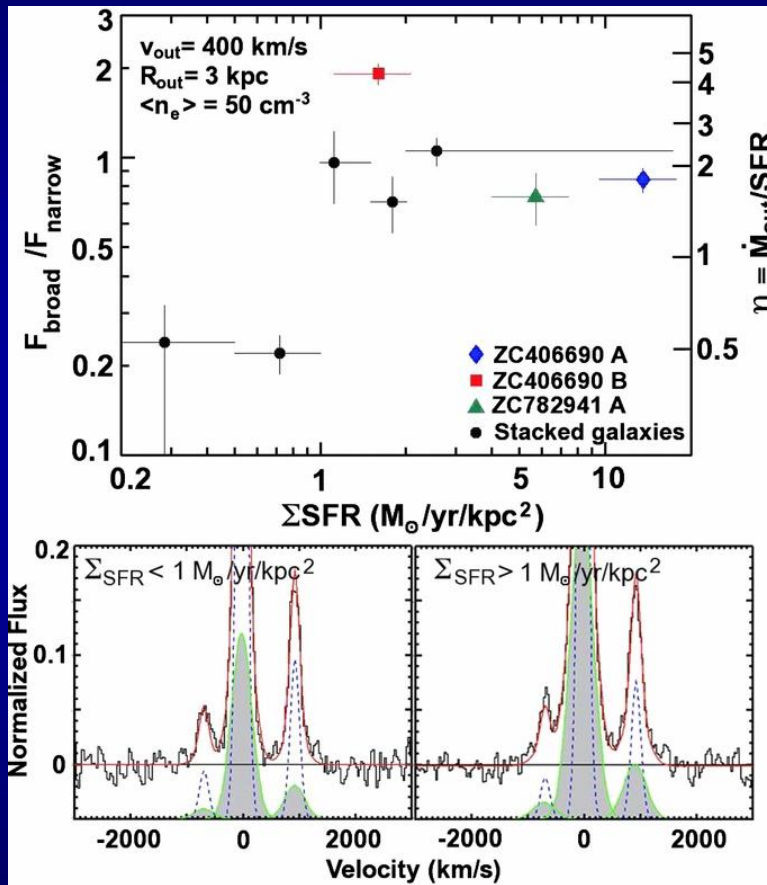


- 72 galaxies in the EGS field with Keck/LRIS spectra.
- Outflow speed and Σ_{SFR} are correlated at $>3\sigma$
- Composite spectra show the same effect (MgII)
- See also Bordoloi et al. (2013)



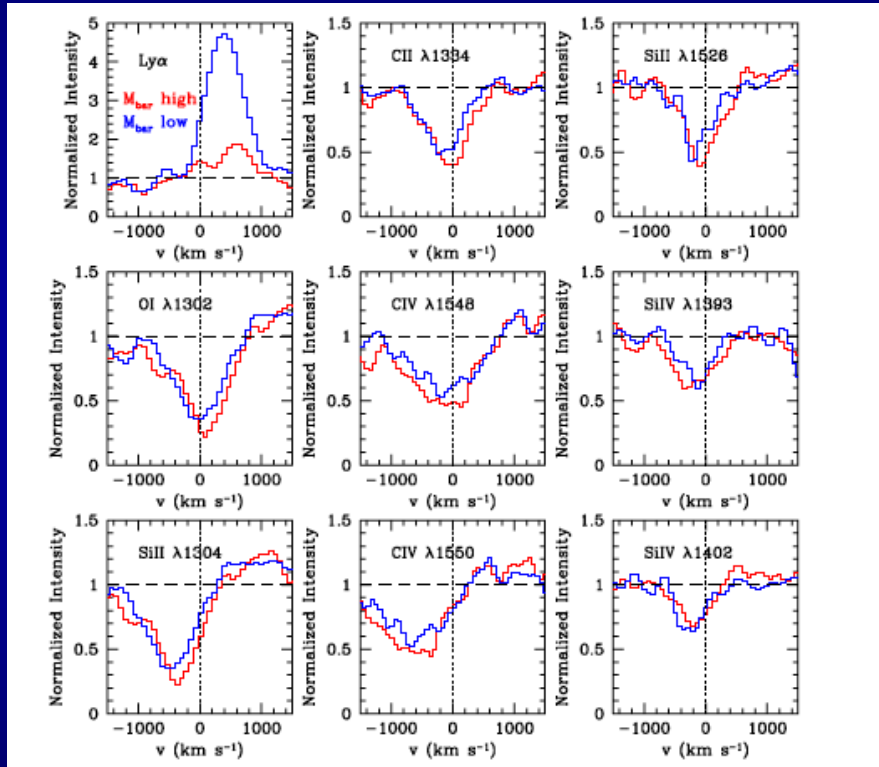
(Kornei, AS et al. 2012)

Outflow kinematics at $z \sim 2$



- 27 galaxies with SINFONI IFU H α spectra.
- Strongest correlation of broad flux fraction with Σ_{SFR} .
- Also find that more massive, smaller, higher-SFR, face-on galaxies have larger broad flux fraction. But Σ_{SFR} connection is the strongest.
- Suggest Σ_{SFR} threshold for wind breaking out, $\sim 1 M_{\text{sun}}/\text{yr}/\text{kpc}$

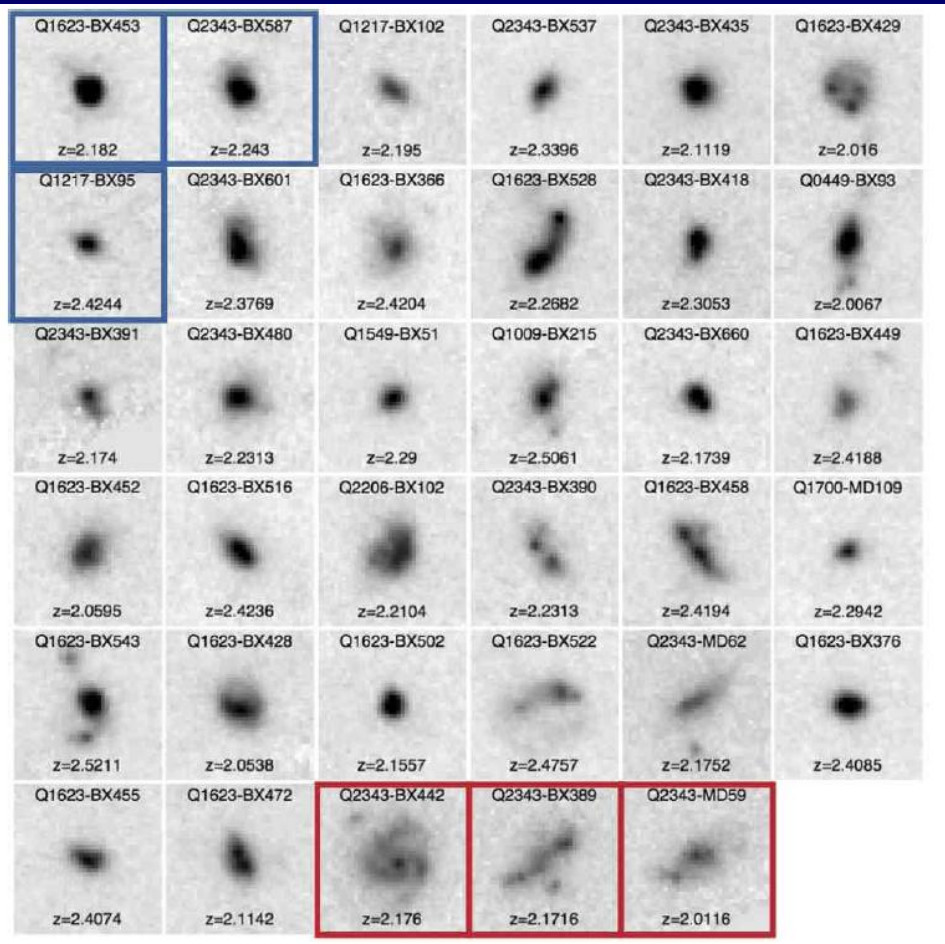
Outflow kinematics at $z \sim 2-3$



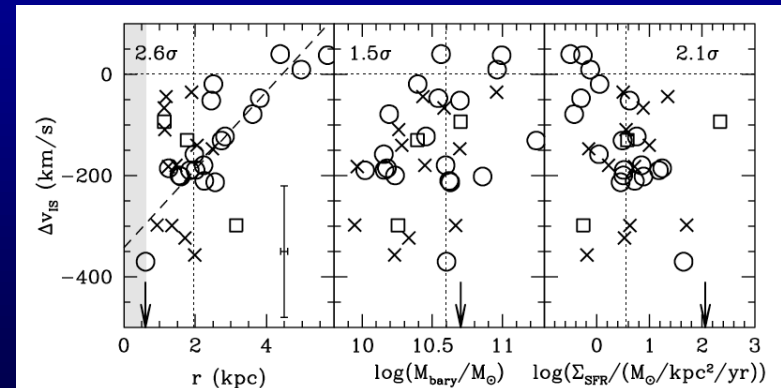
(Steidel et al. 2010)

- Sample of 89 galaxies with rest-frame optical spectra, stellar and gas (stellar+gas=total baryonic) mass estimates. Strongest trend is between $|v_{\text{out}}|$ and M_{bar} , with smaller $|v_{\text{out}}|$ for larger M_{bar}
- Construct low and high M_{bar} samples. Find that blue wings of profiles are identical, with $|v_{\text{max}}| \sim 800$ km/s. High M_{bar} sample is characterized by stronger absorption component at $v_{\text{out}} > \sim 0$. Infalling material? Law et al. (2012c) find that galaxies with large radius have stronger $v \sim 0$ component as well.

Outflow kinematics at $z \sim 2-3$

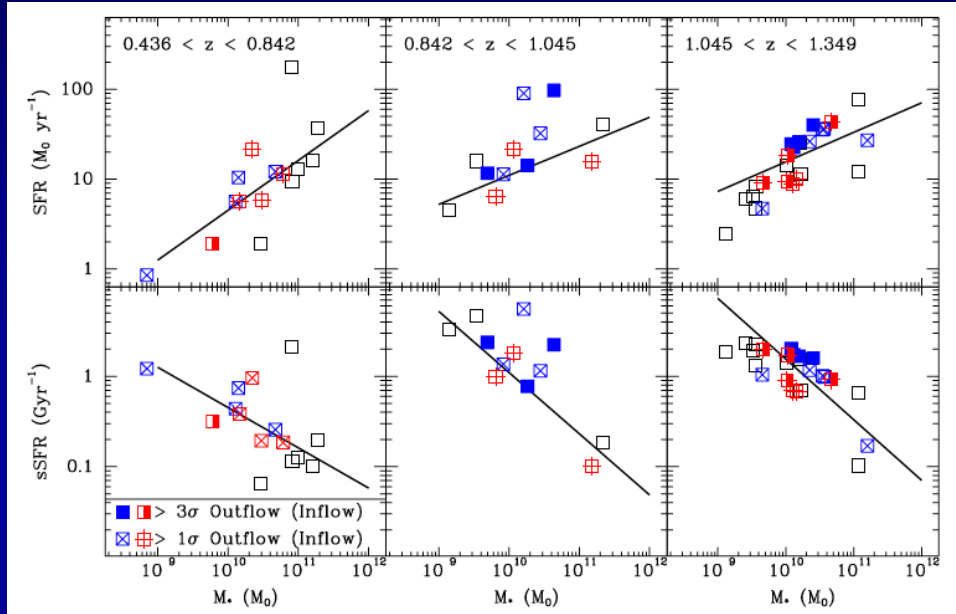


- Law et al. (2012c) use sample of 35 galaxies w/ HST/WFC3, rest-UV spectra, and systemic redshifts.
- Galaxies with large radius have stronger $v \sim 0$ component as well (strongest correlation).
- 2.1σ correlation between absorption velocity centroid and Σ_{SFR} .
- No evidence for correlation between outflow speed and inclination.



(Law et al. 2012c)

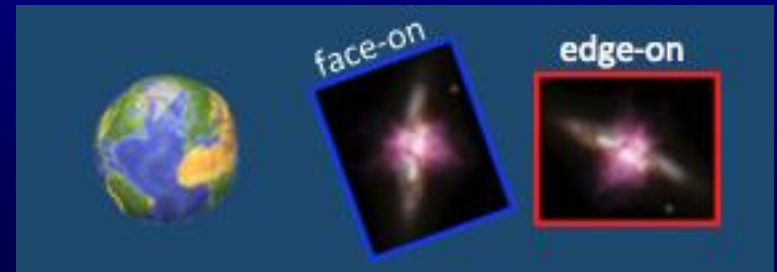
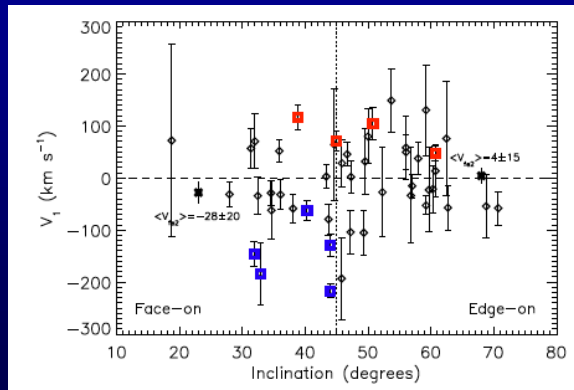
Outflow Geometry at $z \sim 1$



- Outflows detected in $\sim 40\%$ of DEEP2/LRIS sample at $z \sim 1$.
- Outflow detection relatively independent of galaxy properties.
- Outflows more common in face-on systems (Kornei, AS et al. 2012; Bordoloi et al. 2013)
- $z \sim 1$ outflows are collimated!!
- With detection fraction $\Omega/4\pi$:

$$\Omega = 4\pi(1 - \cos \theta_B),$$

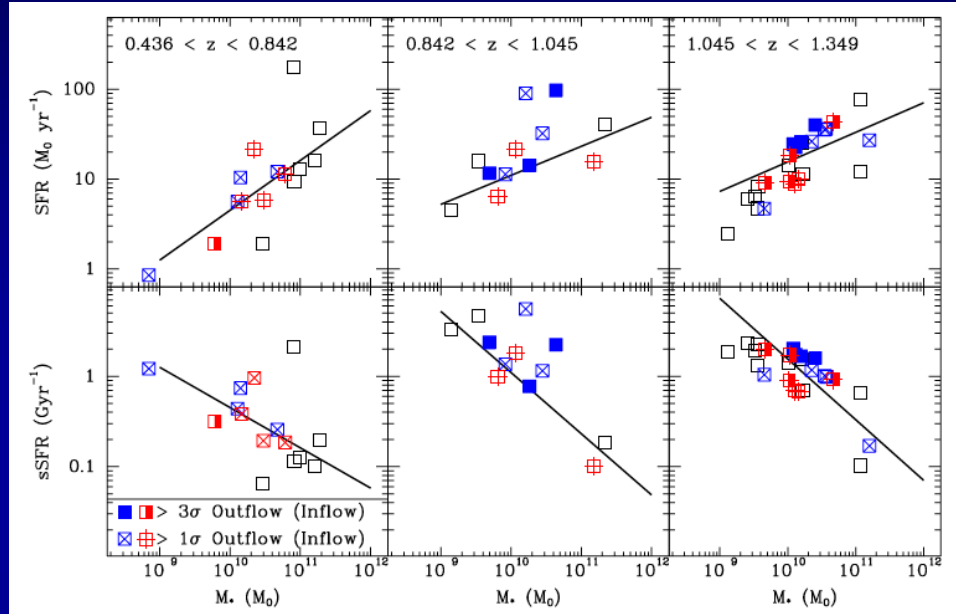
where $\theta_B = \text{cone half angle}$



(Martin, AS et al. 2012)

(Kornei, AS et al. 2012)

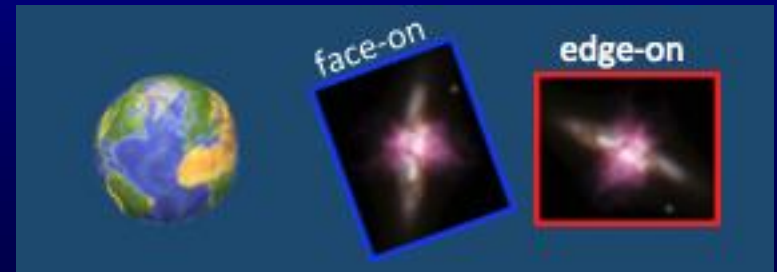
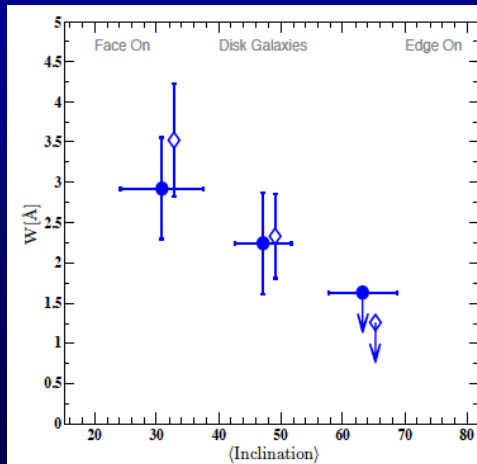
Outflow Geometry at z~1



- Outflows detected in ~40% of DEEP2/LRIS sample at z~1.
- Outflow detection relatively independent of galaxy properties.
- Outflows more common in face-on systems (Kornei, AS et al. 2012; Bordoloi et al. 2013)
- z~1 outflows are collimated!!
- With detection fraction $\Omega/4\pi$:

$$\Omega = 4\pi(1 - \cos \theta_B),$$

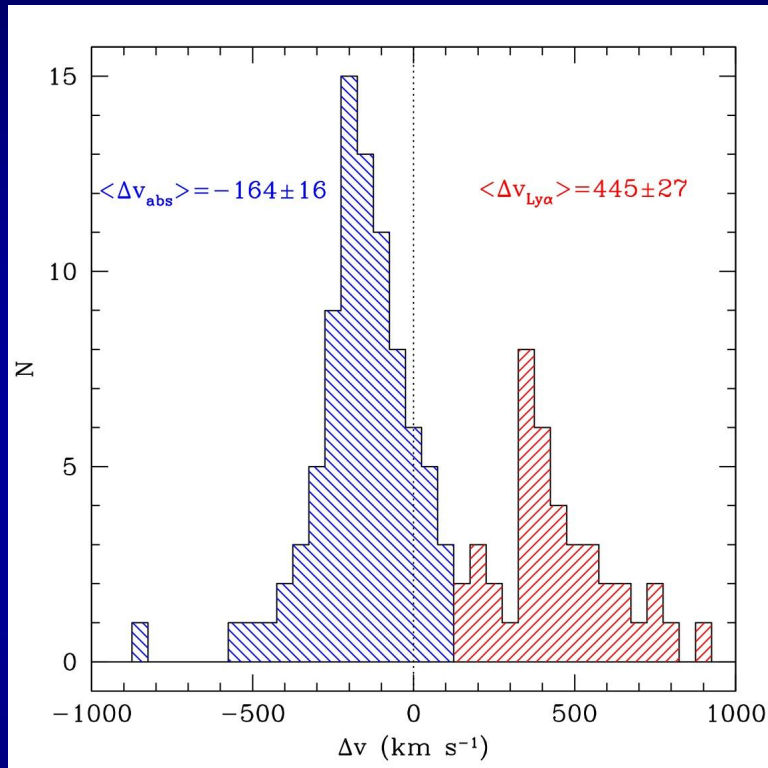
where θ_B =cone half angle



(Martin, AS et al. 2012)

(Bordoloi et al. 2013)

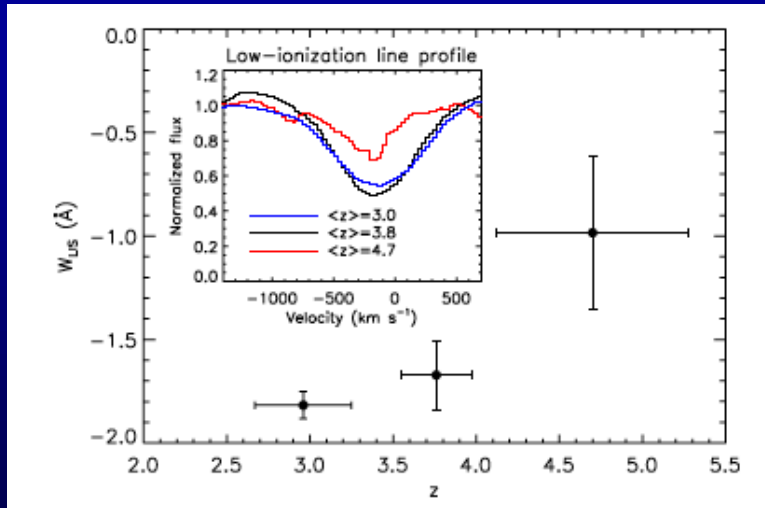
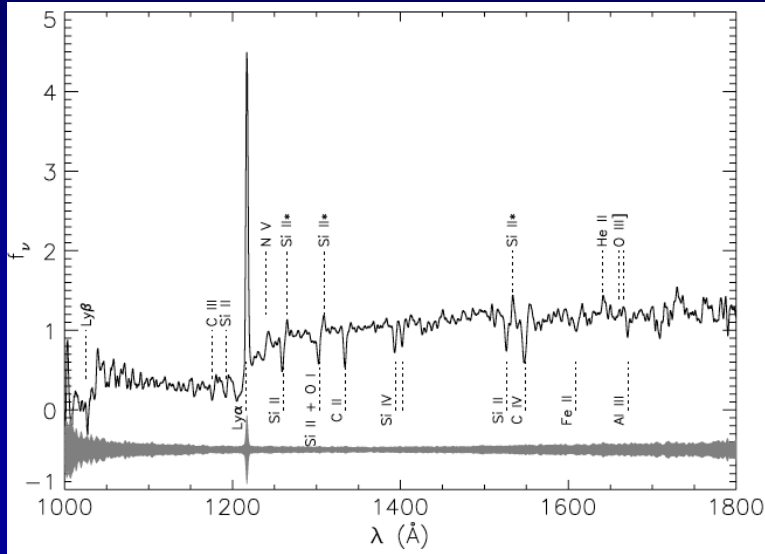
Evolution in Outflow Geometry



(Steidel et al. 2010)

- Outflow signature detected in almost all $z > 2$ LBGs (in contrast to lower- z result).
- Law et al. (2012c) found no correlation between v_{out} and inclination.
- Suggests $z > 2$ outflows are not collimated! More spherical in geometry?
- Related to emergence of disks at $z \sim 1.5$?
- NB: Newman et al. (2012b) find difference in H α broad flux fraction as a function of inclination.

Evolution from $z \sim 4$ to $z \sim 3$

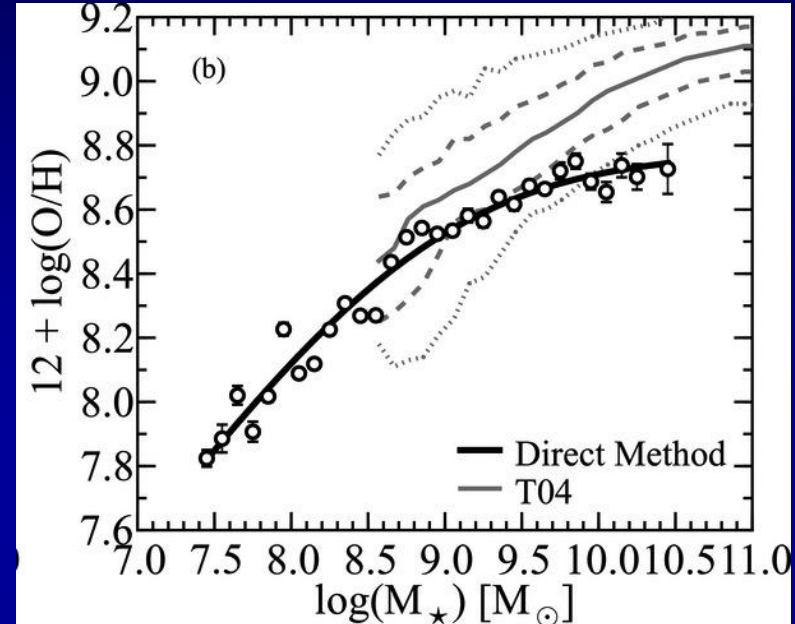
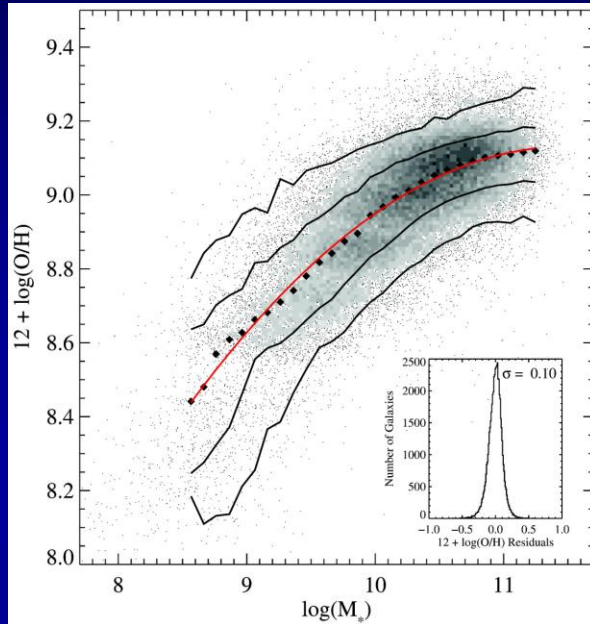


(Jones et al. 2012)

- Sample of 81 at $3.5 < z < 4.5$ with Keck/DEIMOS or VLT/FORS spectra.
- Construct composite, which shows broad, blue-shifted IS absorption.
- For fixed Ly α EW and M_{UV} , galaxies at $z \sim 4$ have lower IS absorption EW than at $z \sim 3$.
- Evolution in spatial distribution, kinematics, covering fraction, optical depth?
- Other evidence that circumgalactic gas is less extended at $z \sim 4$ than $z \sim 3$: SiII* fine structure lines stronger at $z \sim 4$ than at $z \sim 3$.

Mass-Metallicity Relation

(Tremonti et al. 2004)

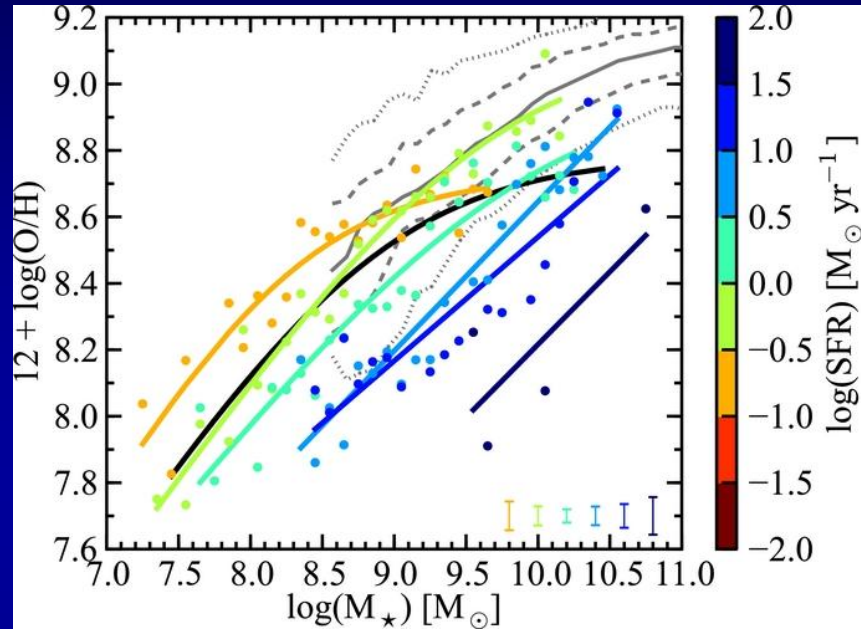
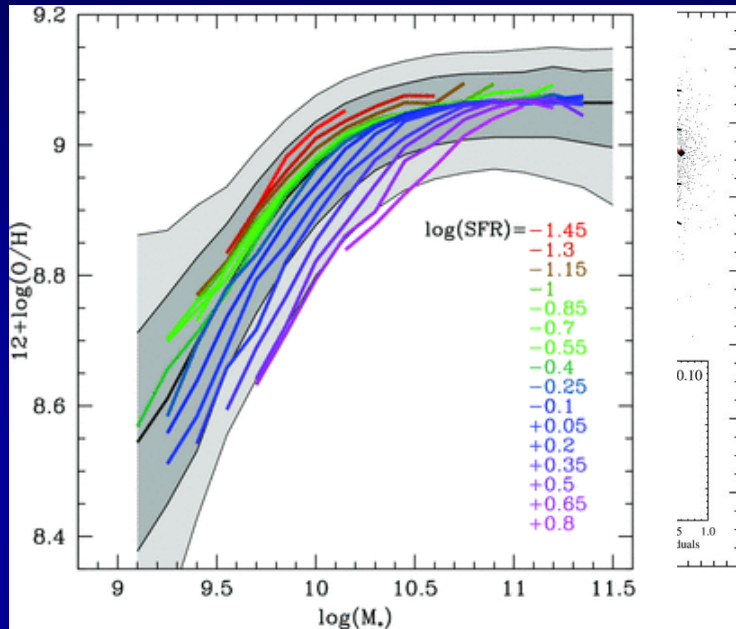


(Andrews & Martini 2013)

- Metal content of galaxies reflects the past integral of star formation, modified by the effects of gas inflow (i.e., accretion) and outflow (i.e., feedback).
- “Metallicity” here means O/H gas-phase abundance.
- Consider together with stellar masses (M-Z relation), gas masses and SFRs (Fundamental Metallicity Relation.)
- Slope, normalization, and scatter in MZR, FMR, place constraints on models of gas outflow/inflow (e.g., Finlator & Dave 2008; Dave et al. 2012)!

Mass-Metallicity Relation

(Mannucci et al. 2010)

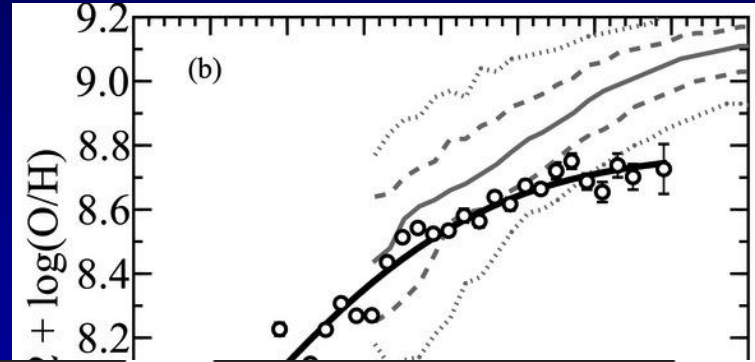
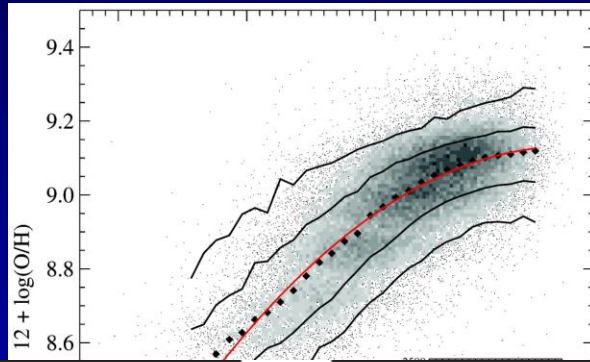


(Andrews & Martini 2013)

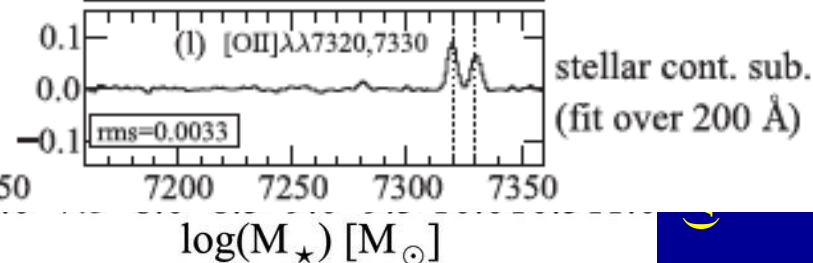
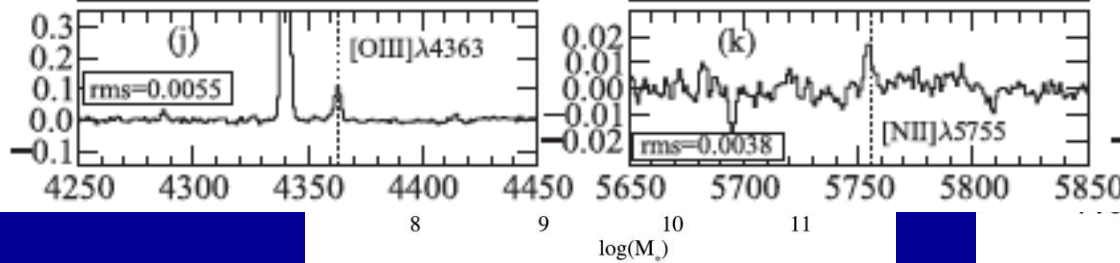
- Metal content of galaxies reflects the past integral of star formation, modified by the effects of gas inflow (i.e., accretion) and outflow (i.e., feedback).
- “Metallicity” here means O/H gas-phase abundance.
- Consider together with stellar masses (M-Z relation), gas masses and SFRs (Fundamental Metallicity Relation.)
- Slope, normalization, and scatter in MZR, FMR, place constraints on models of gas outflow/inflow (e.g., Finlator & Dave 2008; Dave et al. 2012)!

Mass-Metallicity Relation

i et al. 2004



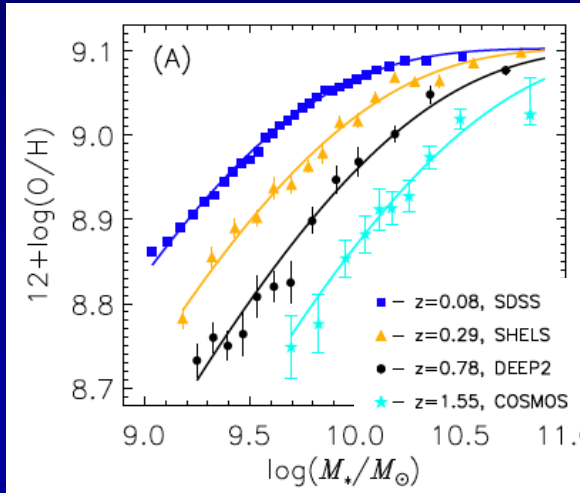
Martini 2013



- New SDSS results from Andrews & Martini (2013) make use of “direct” oxygen abundances in stacked spectra – rather than empirical calibration.
- If $Z_{\text{ISM}} \approx y/(1+\eta)$, new SDSS MZR suggests η scales as $M_*^{-1/2}$ at low-mass end.
- Also obtain constraints on scaling of metal outflow rate (ζ) with M_* (much higher at lower stellar mass).
- Scatter in MZR may indicate time scale for equilibration following gas accretion event, merger, starburst.

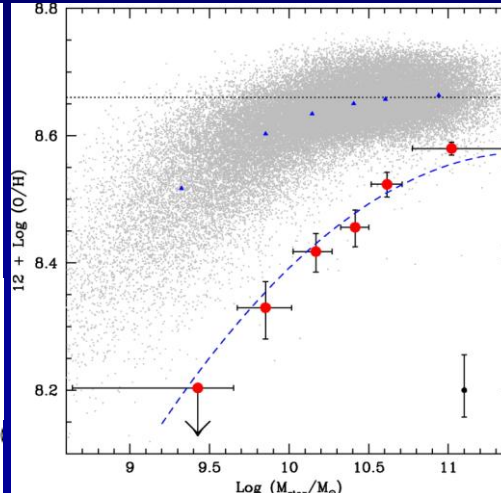
The MZR at High-z

$z=0-1.6$



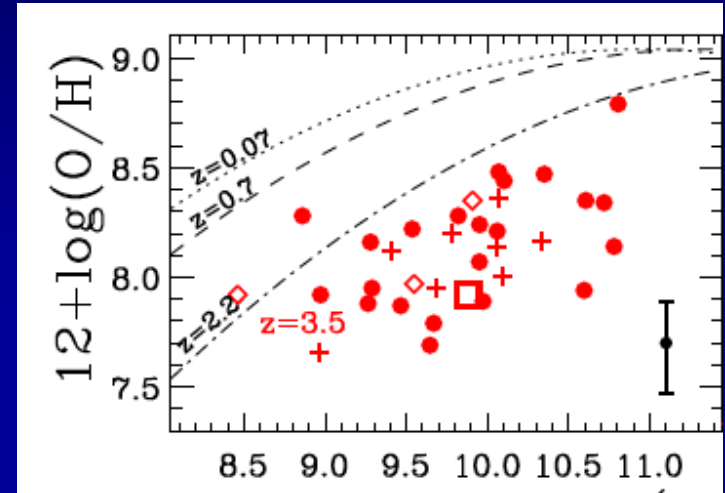
(Zahid et al. 2014)

$z=2.2$



(Erb et al. 2006a)

$z=3.5$



(Troncoso et al. 2014)

- Samples of objects at $z > 1$ with individual M-Z measurements are small, while the stacked samples at, e.g., $z = 2.2$, mask the scatter in the relation.
- Lots of new $z > 1$ data coming in!
- So, how do we estimate O/H at high redshift, given that we can't make "direct" measurements like Andrews & Martini (2013)?

Rest-frame Optical Spectra

- Emission-line set: [OII], H β , [OIII], H α , [NII], [SII]

- Ratios of emission lines used to infer a wide range of physical conditions:

- SFR
{Balmer lines}

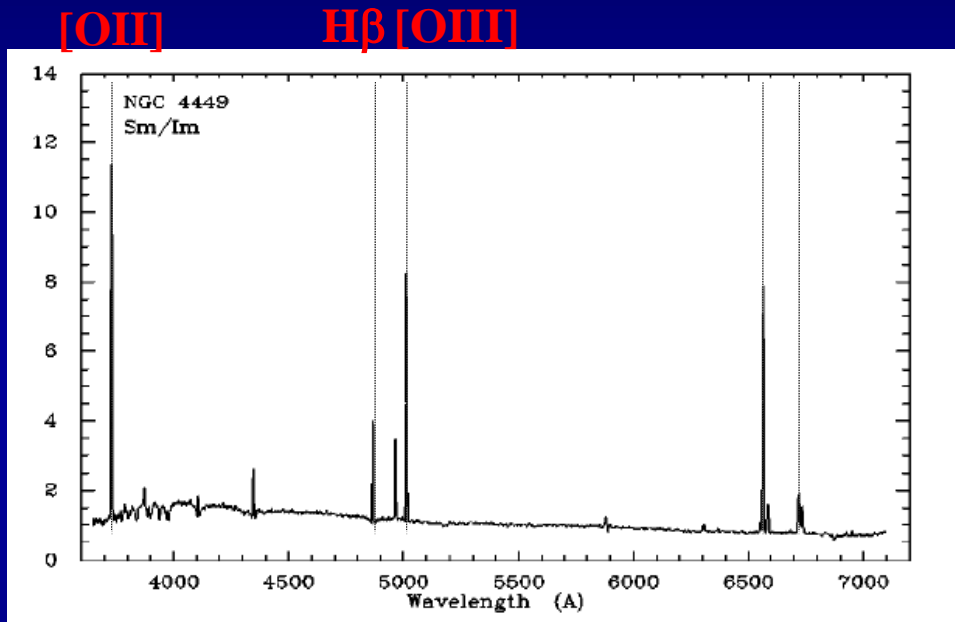
- Metallicity (oxygen)
{R₂₃, N2, O3N2, others}

- Electron density
{[OII] and [SII] doublet ratios}

- Ionization parameter
{[OIII]/[OII]}

- Electron temperature
{[OIII] ratios}

- Dust extinction
{Balmer line ratios}

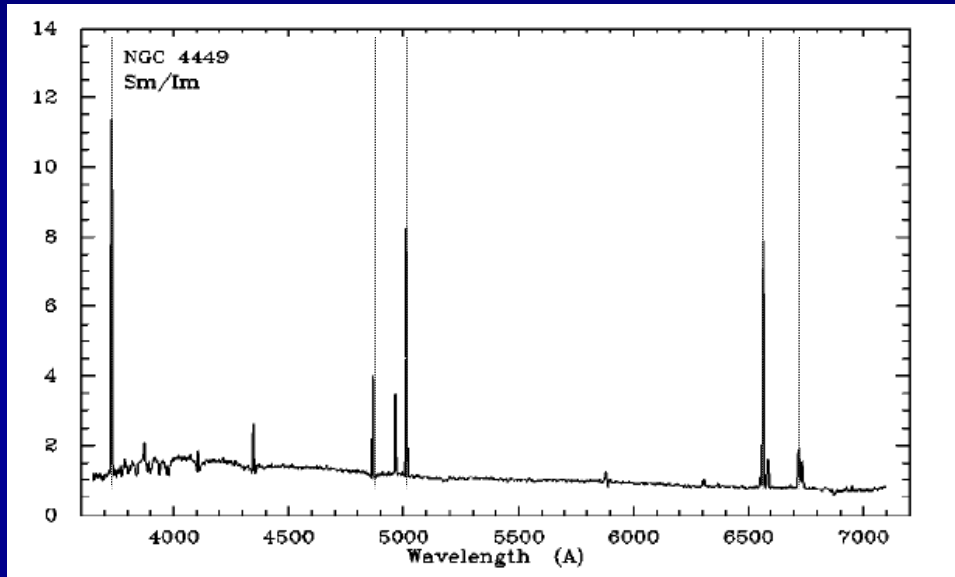


(Kennicutt 1998)

Rest-frame Optical Spectra

- Emission-line set: [OII], H β , [OIII], H α , [NII], [SII]
- Ratios of emission lines used to infer a wide range of physical conditions:

H α +
[NII]



(Kennicutt 1998)

- SFR
{Balmer lines}
- Metallicity (oxygen)
{R₂₃, N2, O3N2, others}
- Electron density
{[OII] and [SII] doublet ratios}
- Ionization parameter
{[OIII]/[OII]}
- Electron temperature
{[OIII] ratios}
- Dust extinction
{Balmer line ratios}

Rest-frame Optical Spectra

- Emission-line set: [OII], H β , [OIII], H α , [NII], [SII]

- Ratios of emission lines used to infer a wide range of physical conditions:

- SFR

{Balmer lines}

- Metallicity (oxygen)

{R₂₃, N2, O3N2, others}

- Electron density

{[OII] and [SII] doublet ratios}

- Ionization parameter

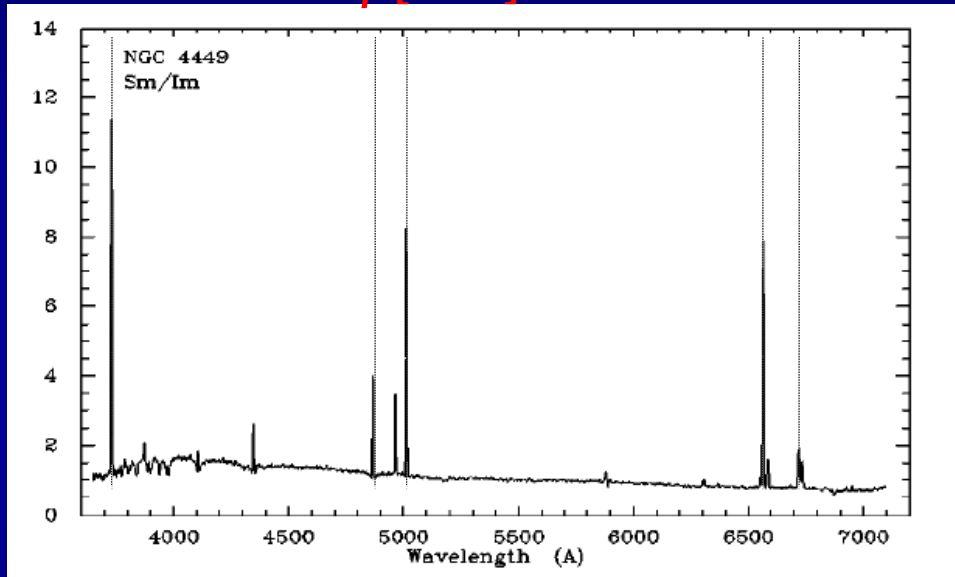
{[OIII]/[OII]}

- Electron temperature

{[OIII] ratios}

- Dust extinction

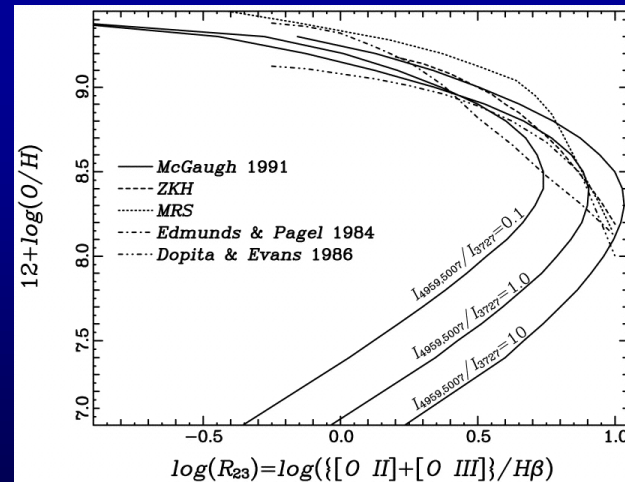
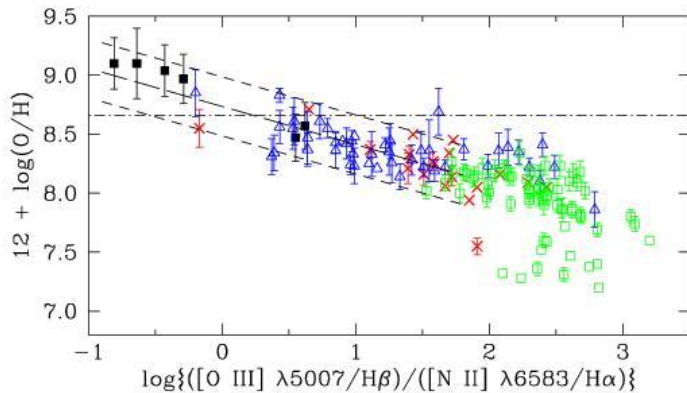
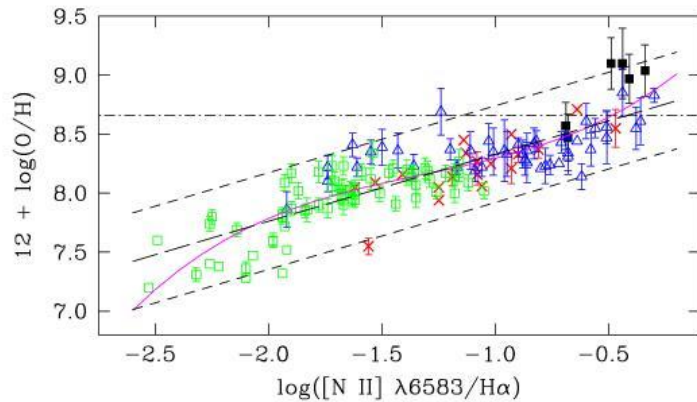
{Balmer line ratios}



(Kennicutt 1998)

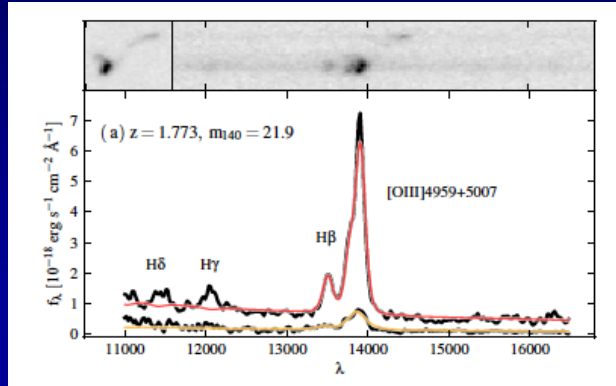
Common Metallicity Indicators

- Subsets of strong, rest-frame optical emission lines have been calibrated against “direct” methods, and photoionization models for local galaxies.



(Pettini & Pagel 2004)

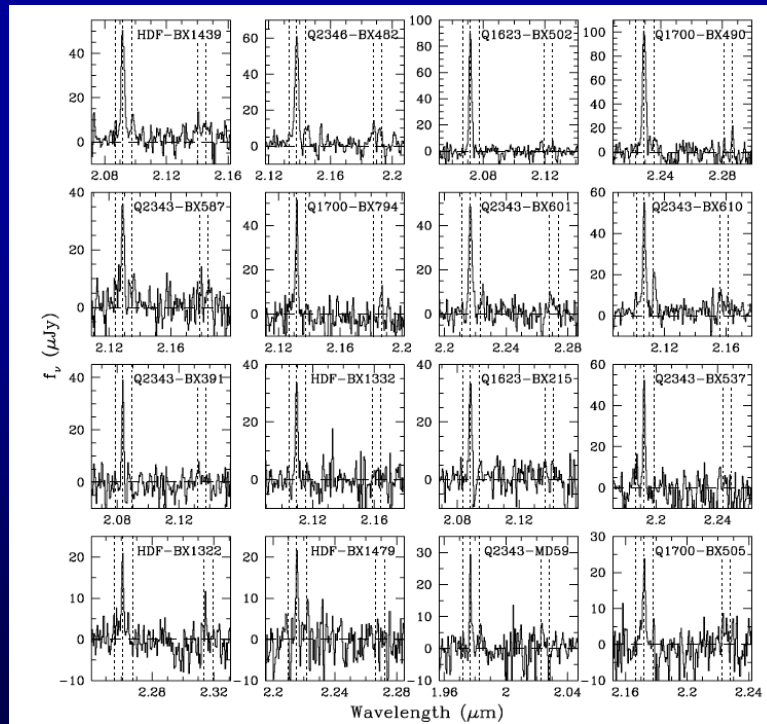
Spectroscopy at $z > 1.5$



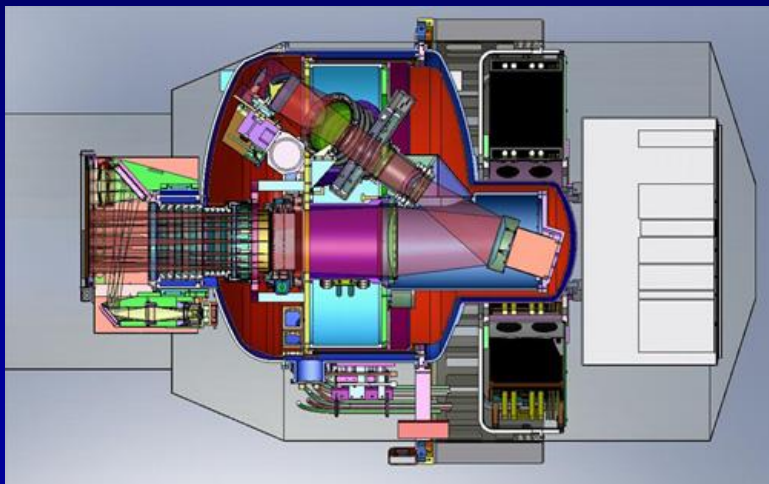
- With the HST WFC3/IR grism, new surveys of $\sim 10,000$ galaxies with rest-frame optical spectroscopy for full range of galaxy types (3D-HST, WISP).

- Low resolution ($R \sim 130$, i.e. $> 2,000 \text{ km/s}$), limited wavelength range ($\lambda < 1.6 \mu\text{m}$).

- Samples of moderate ($R > 1000$) resolution spectra at these redshifts are very small, and typically for one near-IR filter at a time (e.g., Erb et al. 2006).



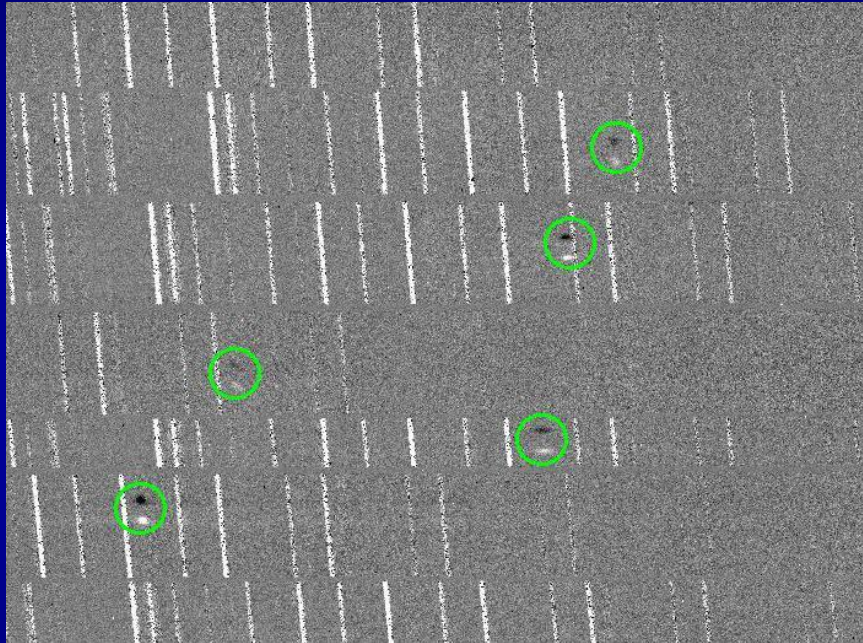
Keck/MOSFIRE



- **Keck/MOSFIRE: Multi-Object Spectrometer for Infra-Red Exploration; co-Pis: McLean (UCLA) and Steidel (Caltech)**
- **Near-IR (0.9-2.5 μm) spectroscopy over 6.1' \times 3.0' FOV, one band (YJHK) at a time, multiplex advantage up to 46 slits using robotic, cryogenic configurable slit unit. $R=2300-3300$ with 0.7" slit .**
- **Commissioned in spring 2012 on the Keck I telescope.**
- **Measurements of rest-frame optical spectra for $z=0.5-5$ galaxies.**



Keck/MOSFIRE



- Sensitivity boost of at least a factor of ~5 relative to previous Keck instrumentation (NIRSPEC).
- Emission-line sensitivities of few $\times 10^{-18}$ erg/s/cm² in 2 hours.
- In practice, typical multiplexing of 30-35.
- Increase in survey efficiency of >2 orders of magnitude!!!!



The MOSDEF Survey

- **Key requirements for an evolutionary census of the galaxy population at $z \sim 1.5-3.5$:**
 - 1. Rest-frame optical spectroscopy covering all of the strongest rest-frame optical emission/absorption features (3700-7000 Å).**
 - 2. A large ($N > 10^3$) sample of objects, spanning the full diversity of stellar populations.**
 - 3. Multiple redshift bins to enable evolutionary studies.**

The MOSFIRE Deep Evolution Field (MOSDEF) Survey achieves these goals.

The MOSDEF Survey

The MOSFIRE Deep Evolution Field Survey



Co-PIs (in alphabetical order):

Alison Coil (UC San Diego)
Mariska Kriek (UC Berkeley)
Bahram Mobasher (UC Riverside)
Naveen Reddy (UC Riverside)
Alice Shapley (UC Los Angeles)
Brian Siana (UC Riverside)

Students:

William Freeman (UC Riverside)
Sedona Price (UC Berkeley)
Ryan Sanders (UC Los Angeles)
Irene Shivaiei (UC Riverside)

Theory Co-Is:

James Bullock (UC Irvine)
Charlie Conroy (UC Santa Cruz)
Romeel Dave (University of Western Cape)
Dusan Keres (UC San Diego)
Marc Krumholz (UC Santa Cruz)

Collaborators

James Aird (Durham University)

The MOSDEF Survey

• Large UO

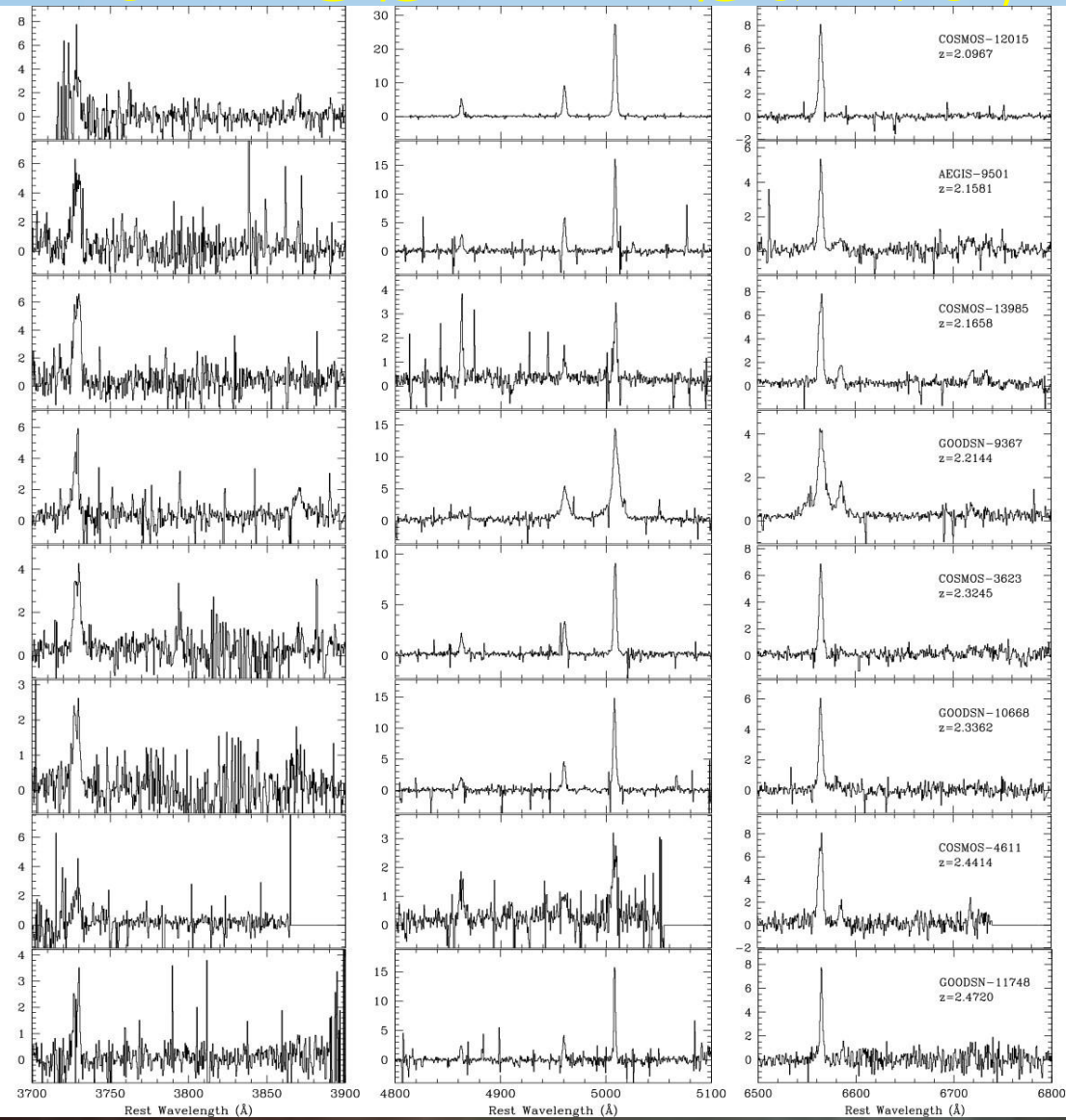
S
2
•
V
2
•

z~2.5; ~50

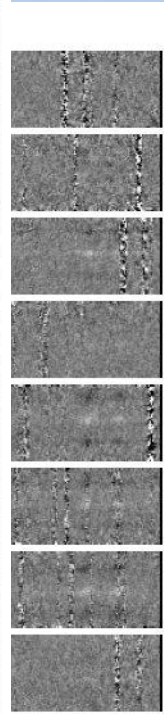
• Target se
optical lun

gn2_05_7979	z=2.207
gn2_05_8072	z=2.235
gn2_05_9766	z=2.194
ae2_03_1361	z=2.184
ae2_03_905	z=2.188
co2_03_13899	z=2.187
co2_03_13985	z=2.166
co2_03_10701	z=2.195

Flux Density (10^{-18} erg/s/cm²/ang)



ddy, Coil,



m

already.

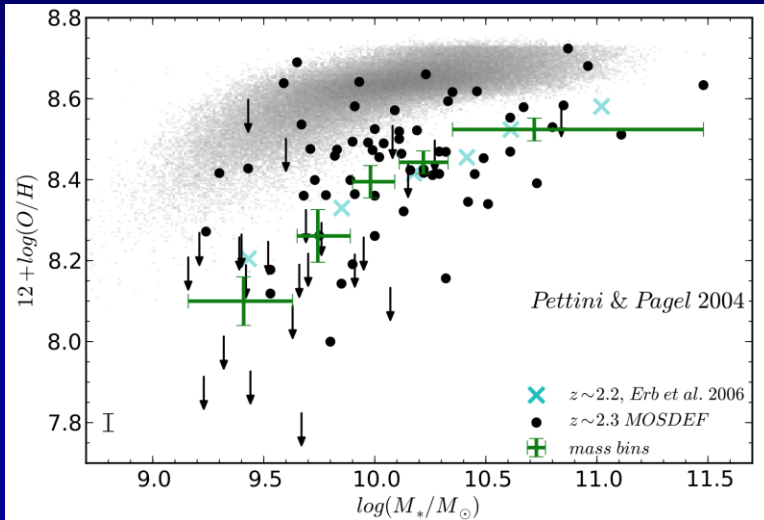
ame

les.

The MOSDEF Survey: Science

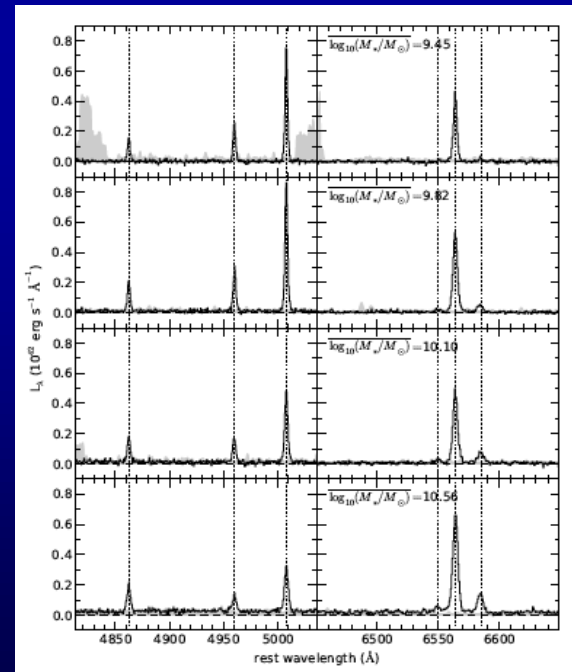
- Star formation and the growth of galaxies
- Dust attenuation
- **Metallicities and physical conditions (density, excitation)**
- The cycle of baryons (outflows, inflows)
- Dynamical masses and structural evolution
- AGN accretion and BH/Galaxy co-evolution

The MOSDEF Survey: MZR

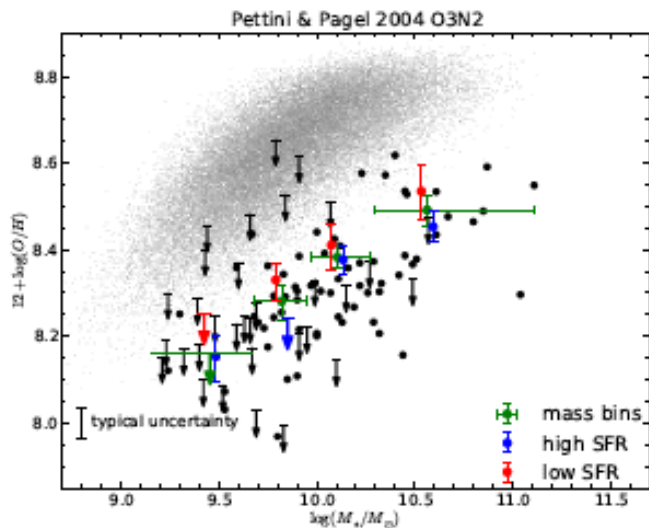
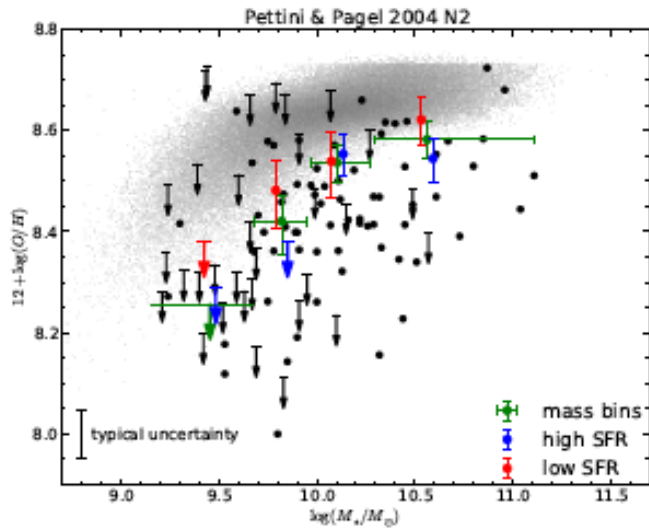


(Sanders, Shapley et al. 2014)

- We have assembled “N2” and “O3N2” metallicities for our $z \sim 2$ MOSDEF sample.
- Detect well-known offset towards lower metallicity at fixed mass.
- Scatter!
- Fair sample at $z \sim 2$.



The MOSDEF Survey: MZR

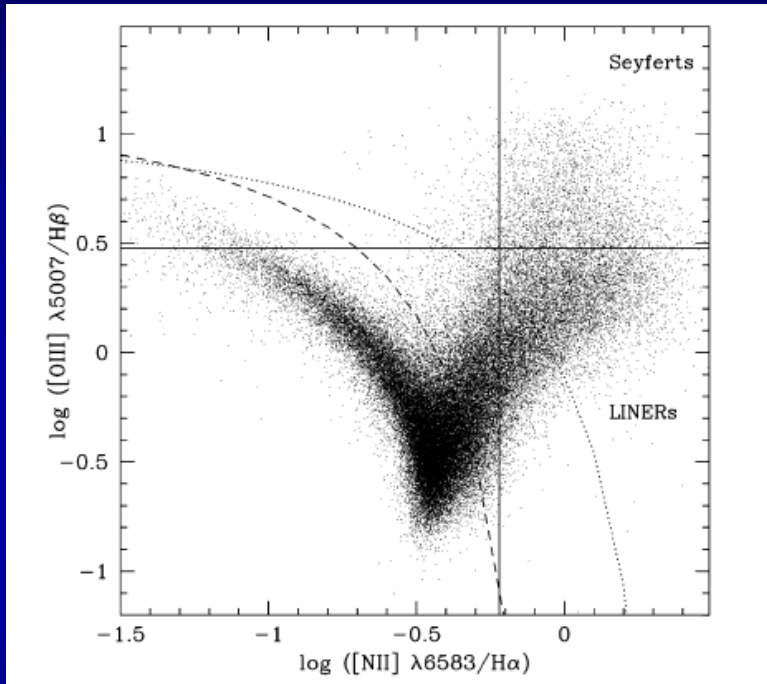


- We don't consistently detect the "FMR" seen at low redshift, with higher-SFR galaxies offset towards lower metallicity at fixed mass.
- Results depend on calibration, inclusion of limits.
- Also need to consider division of sample along SFR, bin in stellar mass.
- There may be issues with using locally-calibrated metallicity indicators....

(Sanders, Shapley et al. 2014)

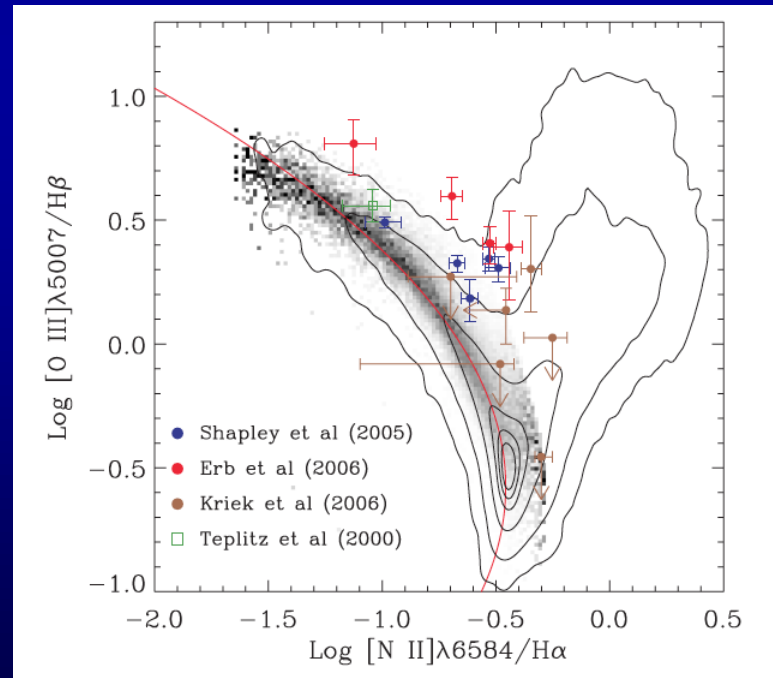
The MOSDEF Survey: BPT

- As we showed several years ago with small samples of objects, $z > 1$ star-forming galaxies are “offset” in the BPT excitation diagram used to separate star-forming galaxies from AGNs.



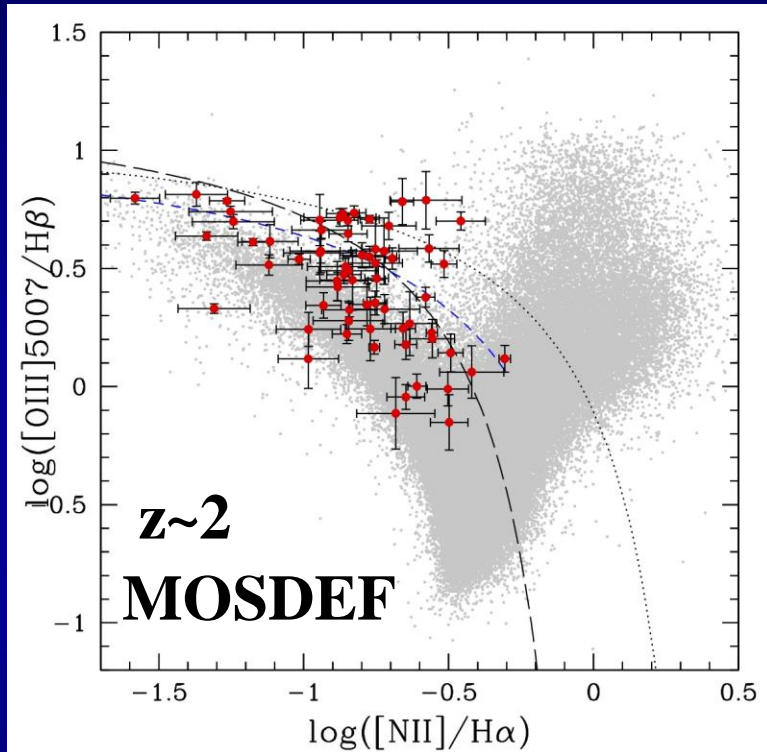
(Kauffmann et al. 2003)

What is the cause of this offset?



(Brinchmann et al. 2008)

The MOSDEF Survey: BPT

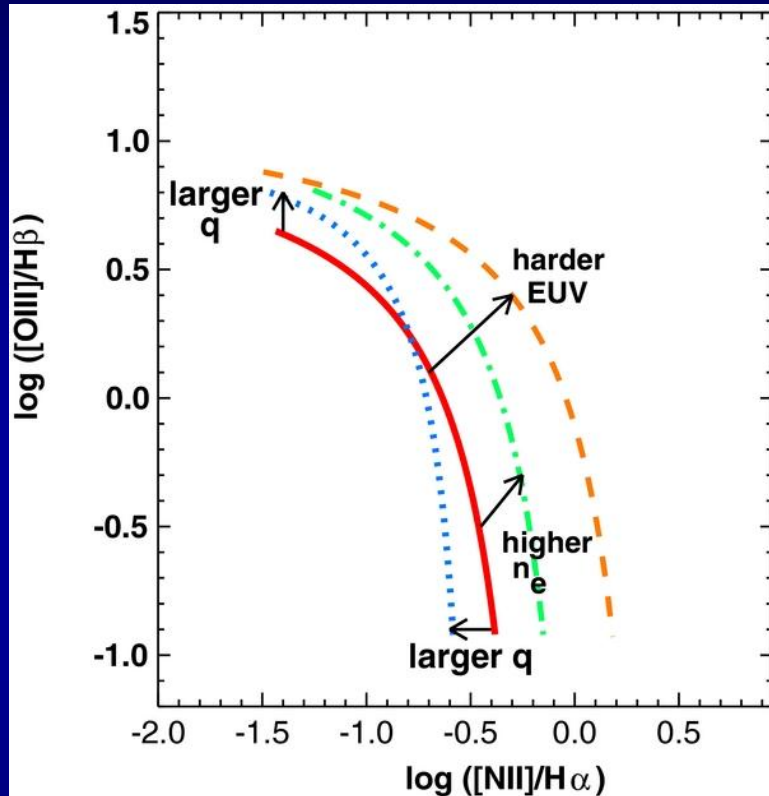


(Shapley et al. 2014)

What is the cause of this offset?

- With a statistical sample already in early MOSDEF data, we can see that the offset is real!
- If line ratios are different in high redshift galaxies, suggests differences in physical conditions in HII regions.
- Higher ionization parameter (geometry of stars relative to gas); harder ionizing radiation field (e.g., Steidel et al. 2014; Kewley et al. 2013).
- With MOSDEF, we will isolate the factors leading to this offset (HII region density, ionization parameter, SFR surface density), and attempt to recalibrate metallicity indicators!

The MOSDEF Survey: BPT

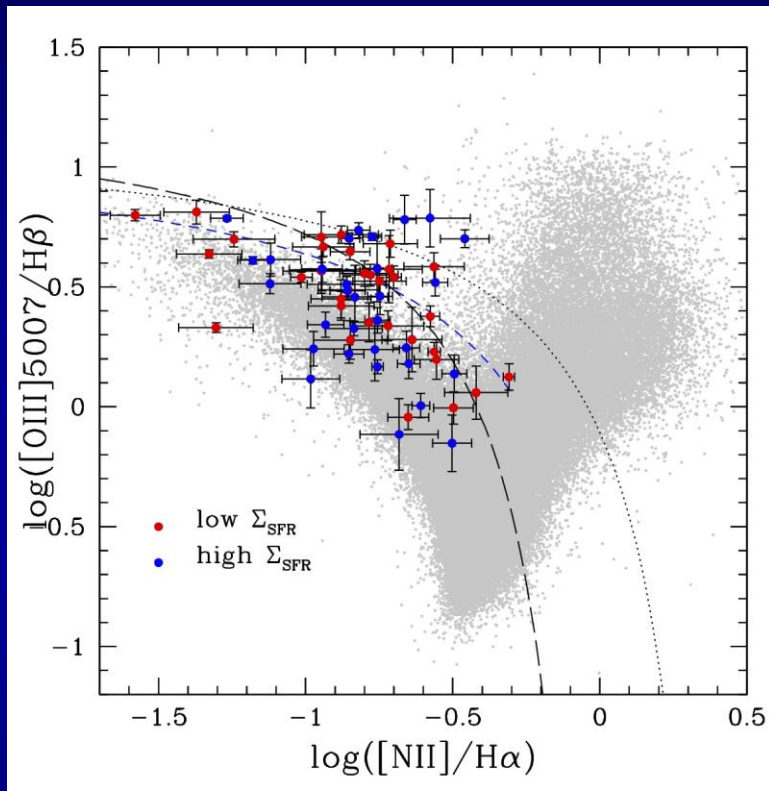


(Kewley et al. 2013)

What is the cause of this offset?

- With a statistical sample already in early MOSDEF data, we can see that the offset is real!
- If line ratios are different in high redshift galaxies, suggests differences in physical conditions in HII regions.
- Higher ionization parameter (geometry of stars relative to gas); harder ionizing radiation field (e.g., Steidel et al. 2014; Kewley et al. 2013).
- With MOSDEF, we will isolate the factors leading to this offset (HII region density, ionization parameter, SFR surface density), and attempt to recalibrate metallicity indicators!

The MOSDEF Survey: BPT

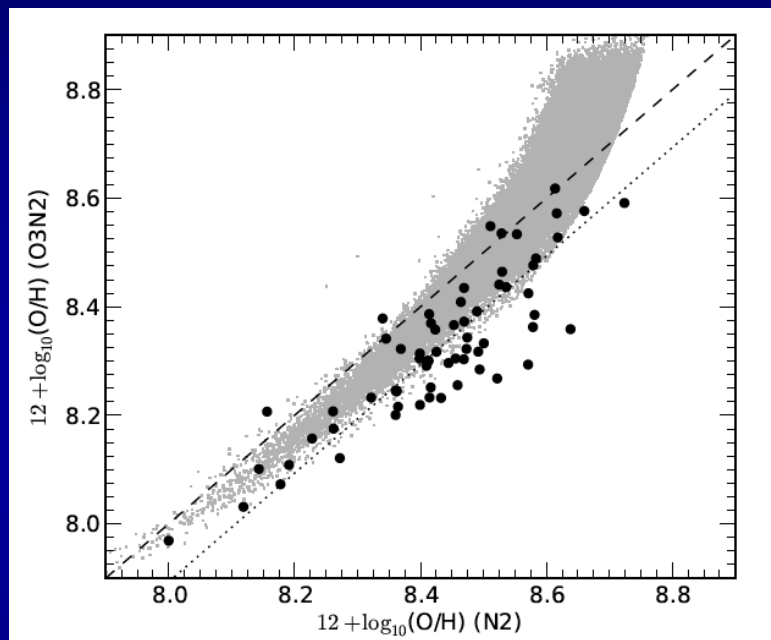


(Shapley et al. 2014)

What is the cause of this offset?

- With a statistical sample already in early MOSDEF data, we can see that the offset is real!
- If line ratios are different in high redshift galaxies, suggests differences in physical conditions in HII regions.
- Higher ionization parameter (geometry of stars relative to gas); harder ionizing radiation field (e.g., Steidel et al. 2014; Kewley et al. 2013).
- With MOSDEF, we will isolate the factors leading to this offset (HII region density, ionization parameter, SFR surface density), and attempt to recalibrate metallicity indicators!

The MOSDEF Survey: BPT



(Sanders et al. 2014)

What is the cause of this offset?

- With a statistical sample already in early MOSDEF data, we can see that the offset is real!
- If line ratios are different in high redshift galaxies, suggests differences in physical conditions in HII regions.
- Higher ionization parameter (geometry of stars relative to gas); harder ionizing radiation field (e.g., Steidel et al. 2014; Kewley et al. 2013).
- With MOSDEF, we will isolate the factors leading to this offset (HII region density, ionization parameter, SFR surface density), and attempt to recalibrate metallicity indicators!

Summary

- Kinematic signatures of outflows at $z \sim 1-4$ are straightforward to establish.
- We can further establish that the geometry of outflows appears to evolve: collimated at $z \leq 1$, not collimated at $z > 2$, and that outflow kinematics are significantly correlated with Σ_{SFR} .
- Outflow physical properties most relevant for models of galaxy formation are very difficult to constrain observationally (e.g., mass/momentum/energy outflow rate, and η , mass loading factor).
- Absorption-line (and emission-line) data with higher spectral resolution will help (lensed galaxies, ; bigger telescopes), as current velocity data are crude and low-resolution.
- The M-Z relation holds promise for placing constraints on outflows, *if we can calibrate metallicity indicators*. **The MOSDEF survey will be key for this.**
- A different approach as well: perhaps better to “observe” simulations and reproduce absorption-line profiles in order to infer mass outflow rates.